Received: 11 March 2022 | Revised: 28 June 2022 | Accepted: 6 July 2022

DOI: 10.1002/dep2.204

The Depositional Record
A journal of the International Association of Sedimentologists
Open Access
IAS
WILEY

REVIEW

Palaeocene to Miocene southern Tethyan carbonate factories: A meta-analysis of the successions of South-western and Western Central Asia

Giovanni Coletti[1] | **Lucrezi Commissario**[1] | **Luca Mariani**[1,2] | **Giulia Bosio**[1] | **Fabien Desbiolles**[1,3] | **Mara Soldi**[4] | **Or M. Bialik**[5]

[1]Department of Earth and Environmental Sciences, University of Milano-Bicocca, Milan, Italy

[2]Departamento de Biologia, Universitat de les Illes Balears, Palma de Mallorca, Spain

[3]CIMA Research Foundation, Savona, Italy

[4]Ecopetrol Srl., Rho, Italy

[5]Marine Geology & Seafloor Surveying, Department of Geosciences, University of Malta, Msida, Malta

Correspondence
Giovanni Coletti, Department of Earth and Environmental Sciences, University of Milano-Bicocca, Piazza della Scienza 4, 20126 Milan, Italy.
Email: giovanni.coletti@unimib.it

Abstract

One hundred and forty-four published successions of shallow-water carbonates, deposited between the Palaeocene and the Miocene, from the Levant to the Himalayas, have been re-analysed using a standardised approach to investigate the distribution of carbonate facies and carbonate-producing organisms. Large benthic foraminifera were found to be the volumetrically most important group of carbonate producers during the whole period, with a peak in abundance during the Eocene. Colonial corals are relatively abundant during the Palaeocene and Miocene, their abundance peaks during the Oligocene and has a minimum during the Eocene. Red calcareous algae have a similar pattern although their peak in abundance covers both the Oligocene and Miocene. Green calcareous algae decrease from the Palaeocene onward. Facies related to very shallow and/or restricted marine conditions peak during the Miocene and in particular during the Aquitanian. Both the pattern of large benthic foraminifera and of colonial corals seems to be related to temperature, with warm periods favouring the former group and cool periods the latter group. Red calcareous algae display a pattern similar to that of colonial corals suggesting that the periods favourable for one group are, on a large scale, also favourable for the other. The progressive decrease of green calcareous alga could be tentatively related to a preservation bias connected to the transition from Palaeogene assemblages that included presumably calcitic taxa of green algae to Neogene assemblages entirely constituted by aragonitic taxa with limited preservation potential. The Aquitanian peak in facies related to very shallow and/or restricted marine conditions is most likely connected to the progressive narrowing of the Tethys related to the collision between Arabia and Eurasia. These results denote an overall agreement between the abundance of the various types of shallow-water carbonate facies and large-scale environmental and geological processes, highlighting the potential for palaeoenvironmental reconstruction locked in the shallow-water record.

KEYWORDS
Asmari Formation, calcareous algae, corals, large benthic foraminifera, Qom Formation, reefs

1 | INTRODUCTION

Earth's biosphere is the result of a complex and ever-changing balance. Biomes can migrate geographically, expand, recede or disappear entirely with new ones arising to take their place. These environmental shifts have been recorded in the fossil record. While many biomes leave limited trace of their existence, others, like tropical carbonate factories, produce massive sedimentary successions that testify to their evolution through time. Carbonate factories represent both the space where biological carbonate sediments are produced and the associations of carbonate-producing organisms (Schlager, 2003; Tucker & Wright, 1990; Wright & Burchette, 1996). Since a sizable share of the benthic organisms inhabiting the biomes of the carbonate factories (e.g. corals, molluscs, calcareous algae, foraminifera) possess a mineralised skeleton, generally either calcite, aragonite or a combination of both, their remains have a high preservation potential and can accumulate in rock-forming quantities. Thanks to this massive and widespread fossil record, it is possible to use carbonate factories as a proxy for studying the changes in the climate of the planet through time (Bosellini & Perrin, 2008; Halfar & Mutti, 2005; Perrin & Bosellini, 2012; Perrin & Kiessling, 2012; Pomar et al., 2017; Wilson, 2008). The distribution of carbonate factories and their palaeoenvironmental implications have been extensively reviewed at both regional and global scale (Halfar & Mutti, 2005; Johnson et al., 2008; Kiessling et al., 1999, 2002; Nebelsick et al., 2005; Pomar et al., 2017). However, these studies often encounter two main limitations. The first is the lack of quantitative data, which significantly hinders any large-scale analysis and accurate comparison of sedimentary successions. The second limitation relates to the geographic distribution of case studies, with the overwhelming majority of well-studied carbonate successions being located in the European area for historical reasons.

This study tries to overcome both of these limitations by compiling a database that summarises the distribution of Cenozoic carbonate facies of South-western and Western Central Asia. With this meta-analysis, the intent is to reconstruct the large-scale patterns of carbonate factories and discuss their palaeoenvironmental implications. This vast region of the world is characterised by extensive carbonate successions deposited during the Cenozoic in the shallow water of the Tethys. The presence of large hydrocarbon reservoirs in these successions (especially in Iran; Amirshahkarami et al., 2007a, 2007b; Coletti et al., 2017; Perry & Choquette, 1985) provides us with a trove of information scattered in individual publications which have not been considered in a larger framework. These papers provide a sizable and invaluable dataset for the investigation of the distribution of carbonate factories and carbonate producers, and to better grasp the global evolution of shelfal biomes during the Cenozoic.

2 | GEOLOGICAL CONTEXT

The regions referred to here as South-western and Western Central Asia consists of land masses mostly located south of the suture line between the African-Arabian and Indian plates and the Eurasian plate (Figure 1). During the Palaeocene to early Miocene, this area was occupied by part of the Tethys Ocean that separated the African, Arabian and Indian landmasses (Gondwanian derived fragments) in the south from the Eurasia in the north (Figure 1). During the entirety of the investigated period (Palaeocene–Miocene) the Tethys Ocean was mainly located at tropical latitudes (Dercourt et al., 2000; Rögl, 1999; Scotese, 2014a, 2014b). This, combined with an overall warm climate punctuated by extremely warm spikes during the early Palaeogene (Barnet et al., 2019; Miller et al., 2020; Zachos et al., 2001), favoured the deposition of shallow-water carbonates (and, at times, evaporites) along Tethys' shelves through most of the investigated time interval. These carbonates formed in a wide variety of environments, ranging from open shelves to restricted embayments and from nutrient-rich to oligotrophic settings, providing a comprehensive overview of the various types of carbonate factories of the Cenozoic.

The northward movement of the African, Arabian and Indian landmasses caused the progressive closure of the Tethys Ocean (Garzanti et al., 2016; Hu et al., 2016; Robertson et al., 2012). The initial collision between the Indian and Eurasian plates took place around 60–61 Ma (An et al., 2021; Hu et al., 2016), leading to the end of marine sedimentation in Tibet and in the Indus Basin (i.e. the western part of the study area) during the Eocene (Afzal et al., 2009, 2011b; Ahmad et al., 2016; Blondeau et al., 1986) (Figure 1). The collision between the Arabian and Eurasian plates probably initiated during the latest Eocene–early Oligocene and was entirely completed before *ca* 14 Ma (middle Miocene) (Agard et al., 2011; Ballato et al., 2010; Bialik et al., 2019;

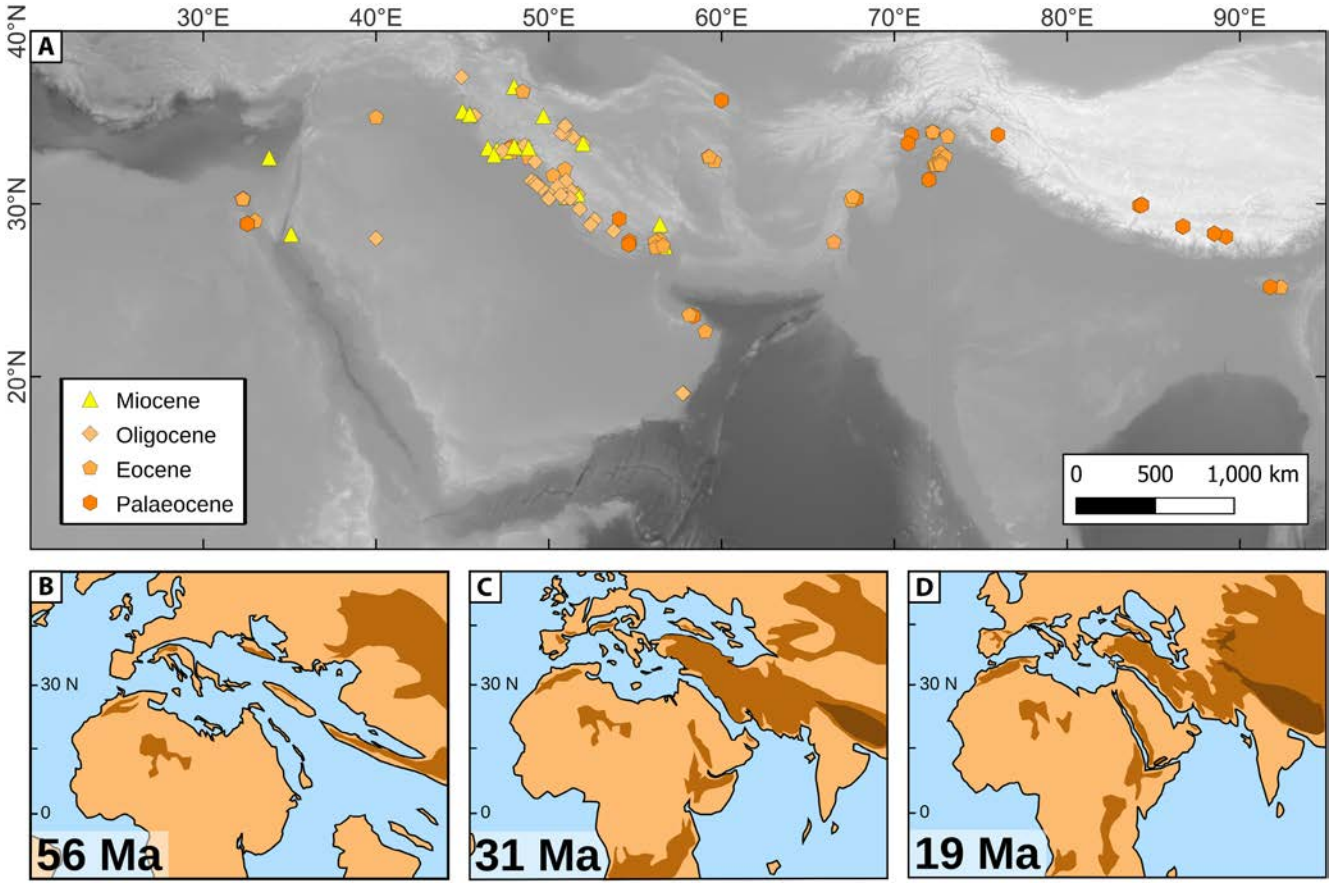

FIGURE 1 Geographic locations of the studied facies and palaeogeographical reconstructions. (A) Geographic location of the fossil Neogene facies investigated in this study. Note the different symbols and colours for different epochs. All the references are reported in Table S1. (B) Palaeogeographical reconstruction of South-western and Western Central Asia about 56 Ma (Palaeocene–Eocene), after Scotese (2014a, 2014b). (C) Palaeogeographical reconstruction of South-western and Western Central Asia about 31 Ma (early Oligocene), after Scotese (2014a, 2014b). (D) Palaeogeographical reconstruction of south-Western and western Central Asia about 19 Ma (early Miocene), after Scotese (2014a, 2014b).

Cornacchia et al., 2018; GholamiZadeh et al., 2021), leading to the end of marine sedimentation in most of the Mesopotamian and Iranian regions (i.e. the central part of the study area) during the Miocene (Al-Juboury & McCann, 2008; Ameen-Lawa & Ghafur, 2015; Mohammadi et al., 2013; Mossadegh et al., 2009; Reuter et al., 2009; Sadooni & Alsharhan, 2019; Sissakian, 2013; Ziegler, 2001) (Figure 1). The Arabian and Levant regions (i.e. the eastern and central part of the study area), during the late Eocene–Oligocene, were also affected by a regional uplift testified by large hiatuses (Agard et al., 2011; Al-Juboury & McCann, 2008; Alsharhan & Nairn, 1995; Avni et al., 2012; Bernecker, 2014; Buchbinder et al., 2005; Coletti et al., 2019; Farouk et al., 2013; Sadooni & Alsharhan, 2019; Whittle et al., 1995). This event has been related to the development of the Afar Dome and the opening of the Red Sea (Avni et al., 2012; Bernecker, 2014; Ziegler, 2001). Both geodynamic processes progressively affected the Tethyan marine environments that are now exposed as outcrops in this vast area running from western Tibet to the south-eastern Mediterranean.

3 | MATERIAL AND METHODS

In order to prepare the database, the main online repositories (e.g. Google Scholar, Scopus) were searched for papers dealing with the Cenozoic carbonate successions of Egypt, Cyprus, Israel, Jordan, Saudi Arabia, United Arab Emirates (UAE), Yemen, Oman, Iraq, Iran, Pakistan, India, Nepal and China (Tibet). To be included into the database, a paper needed to fulfil the following requirements: (1) a lithostratigraphic description of a section completed with a lithostratigraphic column; (2) facies descriptions, including a qualitative or quantitative assessment of the main carbonate producers; (3) information on facies distribution within the investigated section; (4) microphotographs of the recognised facies suitable for double checking facies descriptions; (5) a biostratigraphic or

chronostratigraphic framework; (6) a reasonably accurate location of the investigated section.

The facies described in the selected papers were analysed based on the abundance of the following categories of carbonate grains: free-living larger benthic foraminifera (LBF), encrusting benthic foraminifera (EBF), smaller benthic foraminifera (SBF), red calcareous algae (RCA), green calcareous algae (GCA), colonial corals (CC), molluscs, echinoderms, bryozoans, ostracods, microbial crusts, ooids, peloids and carbonate mud. Each facies was reclassified based on its dominant component (e.g. RCA dominated), or on its codominant components (e.g. RCA and LBF- dominated). Facies dominated by terrigenous grains, pelagic material or evaporites were excluded from the analysis.

Each section included into the database was subdivided into fractions at epoch level (e.g. Eocene, Oligocene) and, wherever possible, at stage level (e.g. Ypresian, Lutetian). Within each fraction of a section, the abundance of each recognised facies was calculated based on how many metres of the fraction are characterised by the facies (e.g. a 40 m fraction of section, deposited during the Ypresian, consists of 20 m of LBF-dominated packstone and of 20 m of ooids-dominated grainstone, thus the fraction of the section consists of 50% of LBF-dominated facies and 50% of ooids-dominated facies). The raw data are available as Table S1.

The data have been grouped based on two different approaches: section-average and formation-average. With the section-average approach, the averages are calculated as the average of each fraction belonging to the same time slice (e.g. the average of all Miocene-aged fractions of sections; the average of all Burdigalian-aged fractions of sections). With the formation-average approach, the averages of all the fractions of sections belonging to the same formation and the same time slice are calculated and then a general average is provided.

Overall, this meta-analysis can be affected by two main biases: the first related to the reliability of the original information and the second related to the geographic distribution of the sections included into the database. The former bias has been partially countered by cross checking both facies descriptions and biostratigraphic information and focussing only on those elements of the facies that were (1) described as dominant and (2) appeared as dominant also in the microphotographs included in the source material. The geographic distribution of the sections is strongly related to the geological setting. While Palaeocene and Eocene sections are more or less evenly distributed into the study area, Oligocene and Miocene sections mainly occur in the Iraq–Iran area (Figure 1A). This is mainly related to the progressive closure of the Tethys Ocean due to the collision of the Indian and African–Arabian plates with Eurasia, which results in the lack of shallow-water carbonate successions in several regions during the Oligocene–Miocene (e.g. Tibet). This geographical bias has been partially countered by proposing both a section-average and a formation-average for each time interval. The section-average approach clearly indicates the average volume of a certain facies among the investigated carbonate successions. This approach provides quantitative data but can over-represents certain areas where there are more investigated outcrops per square kilometre (e.g. the Asmari and Qom Formations of Iran during the Oligo–Miocene interval). The formation-average approach partially solves this problem by averaging the data from each formation, thus reducing the overrepresentation of certain areas. Neither the geographic nor the reliability bias can be entirely solved and must be taken into account when approaching a palaeoenvironmental interpretation of the results.

In order to test whether or not the aforementioned averages are related to large-scale palaeoenvironmental patterns rather than the result of random processes, different statistical procedures were used. Bootstrap analysis was performed on the abundance of the most relevant carbonate facies (i.e. those that constitute the large majority of the analysed sections, i.e. LBF, RCA, CC and GCA dominated and codominated facies). The bootstrap can be used to estimate the precision of an estimated parameter of a population (Efron, 1979). A random sub-sample of the dataset is selected and the parameter is calculated on the sub-sample. The procedure is repeated and the confidence interval of the selected parameter is analysed. A random sub-sample size was selected corresponding to 2/3 (Sengupta et al., 2016) of the original sample (e.g. all the Miocene fractions of sections) and performed 10,000 iterations. A sensitivity analysis was also performed. Since each sub-sample consists of a randomly chosen part of the available fractions of sections of each epoch, the large number of iterations should clarify whether the observed trends in carbonate facies distribution are simply the results of the available group of analysed outcrops. If the distribution of the carbonate facies in the study area during the Cenozoic is not related to large-scale palaeoenvironmental patterns of the planet, one would expect the averages of the various sub-samples to be highly variable, resulting in large and overlapping confidence intervals. On the other hand, if the distribution is indeed the result of large-scale patterns, then the various sub-samples should be relatively homogeneous and the confidence interval on the averages relatively narrow. Multivariate statistics was also used to test the results. If during the Cenozoic, within the study area, the distribution of carbonate factories was random, one would expect the distribution of carbonate facies to be relatively similar during each epoch, with no statistically

significant difference between the various time slices (e.g. no difference between Palaeocene and Miocene distribution of carbonate factories). The analysis was carried out following the recommendations in Bialik et al. (2021) and normal distribution of the variable was tested using Shapiro–Wilk, Anderson–Darlin, Lilliefors and Jarque–Bera tests. PERMANOVA analysis was then carried out to test the dissimilarity between the data of each epoch. Both bootstrap and multivariate statistics were performed on section-averages as formation-averages essentially stem from section-averages.

4 | RESULTS

Some 114 papers providing information on shallow-water carbonate facies from the Palaeocene to the Miocene were identified. Based on the aforementioned requirements, 66 papers and 144 sections, from Cyprus, Egypt, Saudi Arabia, Oman, Iraq, Iran, Pakistan, India and China were included into the database (Table 1; Table S1; the database is also accessible online, https://doi.org/10.6084/m9.figshare.19323821.v1). The remaining papers, although providing qualitative data on the distribution of the main carbonate producers, lacked quantitative information on facies distribution throughout the described sections. The information from this latter group of papers was still included into the discussion.

The sections included into the database range in age from the Palaeocene to the Miocene. The Palaeocene is represented (in order of abundance) by the Thanetian, Danian and Selandian. As the database largely consists of shallow-water carbonates, the stratigraphic framework is strongly reliant upon LBF biostratigraphy. Since LBF zonation is poorly constrained in the Danian–Selandian interval (Serra-Kiel et al., 1998), the pre-Thanetian stratigraphic framework is not well defined. The Eocene is largely represented by the Ypresian stage. Both stages of the Oligocene and both stages of the early Miocene are well represented within the database. On the other hand, the middle and late Miocene are poorly represented. Overall, the various epochs of the database have sample sizes in the same order of magnitude: 42 fractions of sections for the Palaeocene; 61 for the Eocene; 70 for the Oligocene; 85 for the Miocene.

4.1 | Epochs

Photozoan facies (sensu James, 1997), that is those dominated by CC, GCA, LBF and RCA, dominate the carbonate successions of the study area, during the whole Palaeocene-Miocene interval (Table 2; Figure 2). Heterozoan facies (sensu James, 1997), that is those facies mainly dominated by heterotroph carbonate producers like molluscs, echinoderms, SBF and bryozoans, are less common; their combined abundance peaks during the Miocene (Table 2; Figure 2).

The LBF-dominated facies are the most abundant element of the shallow-water carbonates of the study area (Table 2; Figure 3). Overall, taken together, the facies dominated by LBF and the facies codominated by LBF represent the majority of shallow-water carbonates of the Palaeocene, Eocene and Oligocene and Miocene epochs (Table 3; Figure 4). The abundance of LBF peaks during the Eocene and decreases hereafter. The LBF-dominated sections (>90% of the section) persist through all periods. Facies dominated solely by RCA are relatively rare; on the other hand, facies codominated by RCA are rather abundant, usually representing the second or third most abundant facies type (generally after LBF-dominated and LBF-codominated) (Table 2; Figure 3). The RCA codominated facies are relevant during the Palaeocene, Oligocene and Miocene and their abundance is the lowest during the Eocene (Table 2; Figure 3). Taken together CC dominated and CC codominated facies are usually the next most abundant facies type (Table 3; Figure 4). Their abundance peaks during the Oligocene and has a minimum during the Eocene. The GCA facies (either solely considering GCA dominated facies or both GCA dominated and GCA codominated facies) only occur in significant amounts during the Palaeocene and Eocene, being more common in the former (Tables 2 and 3; Figures 3 and 4). All other producers are uncommon for the entire time period (Palaeocene to early Miocene). The EBF facies are very rare in all the epochs except in the Eocene where they account, on average, for 2.5% of section-average fractions (Tables 2 and 3). Microbial crust-dominated facies are extremely rare during every epoch (Tables 2 and 3). Facies characterised by the dominance of non-skeletal grains are relatively rare during the Palaeocene and Eocene and become more common during the Oligocene and Miocene (Tables 2 and 3; Figure 2). Intertidal mud dominated facies occur in every epoch and their abundance peaks during the Miocene where they are one of the most common non-skeletal facies types (Tables 2 and 3).

4.2 | Rupelian–Burdigalian detailed analysis

Since the Palaeocene is mainly represented by Thanetian deposits, the Eocene by Ypresian deposits, and the Miocene by early Miocene deposits, the analysis at stage level was performed only in the Rupelian–Burdigalian interval. As in the epoch analysis, the photozoan

TABLE 1 Summary list of the papers considered in this work, reporting references, countries, formations, stratigraphic ranges and the number of sections analysed in the work. See Table S1 for the complete dataset.

#	Reference	Country	Formation	Stratigraphic range	N. sections
1	Rahmani et al. (2009)	Iran	Asmari	Chattian—Burdigalian	1
2	Adabi et al. (2008)	Iran	Taleh Zang	Lutetian—Bartonian	2
3	Roozpeykar and Moghaddam (2016)	Iran	Asmari	Rupelian—Burdigalian	1
4	Nafarieh et al. (2012)	Iran	Jahrum	Selandian—Ypresian	2
5	Mahyad et al. (2019)	Iran	Qom	Aquitanian—Burdigalian	2
6	Moghaddam et al. (2002)	Iran	Jahrum & Pabdeh	Ypresian	1
7	Heidari et al. (2014)	Iran	Mishan (Guri Member)	Aquitanian—Langhian	2
8	Shabafrooz et al. (2015)	Iran	Asmari	Rupelian—Burdigalian	9
9	Vaziri-Moghaddam et al. (2006)	Iran	Asmari	Chattian—Burdigalian	1
10	Zohdi et al. (2013)	Iran	Jahrum	Ypresian—Bartonian	4
11	Daraei et al. (2015)	Iran	Asmari	early Miocene	3
12	Roozpeykar et al. (2019)	Iran	Asmari	Burdigalian	1
13	Avarjani et al. (2015)	Iran	Asmari	Chattian—Burdigalian	4
14	Bagherpour and Vaziri (2012)	Iran	Taleh Zang	Thanetian—Ypresian	2
15	Amirshahkarami and Zebarjadi (2018)	Iran	Jahrum	Thanetian—Ypresian	1
16	Zoeram et al. (2015)	Iran	Asmari	Rupelian—Burdigalian	1
17	Basso et al. (2019)	Iran	Qom	Rupelian	1
18	Mohammadi et al. (2011)	Iran	Qom	Chattian	1
19	Hadi et al. (2016)	Iran	Ziarat	Ypresian—Bartonian	3
20	Sadeghi et al. (2011)	Iran	Asmari	Rupelian—Chattian	3
21	Amirshahkarami (2013)	Iran	Asmari	Rupelian—Aquitanian	2
22	Vaziri-Moghaddam et al. (2010)	Iran	Asmari	Chattian—Burdigalian	4
23	Amirshahkarami and Karavan (2015)	Iran	Qom	Rupelian—Burdigalian	1
24	Dill et al. (2018)	Iran	Asmari	Rupelian—Burdigalian	5
25	Dill et al. (2012)	Iran	Asmari	Chattian—Burdigalian	1
26	Noorian et al. (2021)	Iran	Asmari	Rupelian—Burdigalian	3
27	Safari et al. (2020)	Iran	Qom	Rupelian—Chattian	2
28	Amirshahkarami et al. (2007a)	Iran	Asmari	Rupelian—Early Miocene	1
29	Babazadeh and Alavi (2013)	Iran	Lut platform	Ypresian	3
30	Taheri et al. (2008)	Iran	Jahrum	Lutetian	1
31	Mossadegh et al. (2009)	Iran	Asmari	Chattian—Burdigalian	2
32	Amirshahkarami et al. (2007b)	Iran	Asmari	Chattian—Early Miocene	1
33	Adabi et al. (2016)	Iran	Asmari	Rupelian—Burdigalian	1
34	Vaziri-Moghaddam et al. (2011)	Iran	Asmari	Rupelian—Chattian	1
35	Mahboubi et al. (2001)	Iran	Chehel- Kaman	Thanetian	2
36	Mohammadi (2020)	Iran	Qom	Rupelian—Burdigalian	2
37	Joudaki et al. (2020)	Iran	Asmari	Rupelian—Burdigalian	2
38	Al-Qayim et al. (2016)	Iraq	Bajwan, Anah, Euphrates, Jeribe	Rupelian—Burdigalian	1
39	Hussein et al. (2017)	Iraq	Euphrates, Jeribe	Aquitanian—Burdigalian	5
40	Swati et al. (2013)	Pakistan	Margalla Hill Limestone	Ypresian	1
41	Afzal et al. (2011a)	Pakistan	Lockhart, Patala, Dungan	Thanetian—Ypresian	5

TABLE 1 (Continued)

#	Reference	Country	Formation	Stratigraphic range	N. sections
42	Fahad et al. (2021)	Pakistan	Chorgali	Ypresian	1
43	Ishaq et al. (2019)	Pakistan	Sakesar Limestone	Ypresian	2
44	Ghazi et al. (2020)	Pakistan	Nammal	Ypresian	6
45	Hanif et al. (2014)	Pakistan	Lockhart	Thanetian	3
46	Ahmad et al. (2020)	Pakistan	Dungan	Thanetian—Ypresian	1
47	Kamran et al. (2021)	Pakistan	Patala	Thanetian—Ypresian	1
48	Kahsnitz (2017)	India	Spanboth, Zhepure Shan, Zongpu, Langzhu	Selandian—Ypresian	5
49	Sarkar (2016)	India	Umlatdoh (Umlatdoh Limestone)	Ypresian	1
50	Sarkar (2017)	India	Prang	Lutetian—Bartonian	1
51	Banerjee et al. (2018)	India	Furla Limestone, Maniyara Fort	Lutetian—Bartonian, Chattian	2
52	Jauhri et al. (2006)	India	Lakadong (Lakadong Limestone)	Thanetian	1
53	Jiang et al. (2021)	China	Jialazi	Thanetian—Ypresian	2
54	Li et al. (2015)	China	Zongpu	Danian—Ypresian	2
55	Li et al. (2020)	China	Not reported (probably Zhepure Shan)	Thanetian—Ypresian	1
56	Willems et al. (1996)	China	Zhepure Shan	Danian—Lutetian	1
57	Mattern and Bernecker (2019)	Oman	Jafnayn	Thanetian—Ypresian	1
58	Tomás et al. (2016)	Oman	Jafnayn	Ypresian	1
59	Beavington-Penney et al. (2006)	Oman	Seeb	Lutetian—Bartonian	1
60	Reuter et al. (2008)	Oman	Shuwayr, Warak, Ghubbarrah	Rupelian—Aquitanian	2
61	Al-Kahtany (2017)	Saudi Arabia	Jabal Kibrit (Wadi Waqb Member)	middle Miocene	1
62	Corlett et al. (2018)	Egypt	Hammam Faraun fault block	Ypresian—Lutetian	1
63	Sallam et al. (2015)	Egypt	Minia, Sannor, Maadi	Ypresian, Bartonian—Priabonian	5
64	Scheibner et al. (2000)	Egypt	Southern Galala	Thanetian	6
65	Scheibner et al. (2003)	Egypt	Southern Galala	Thanetian	4
66	Coletti et al. (2019)	Cyprus	—	Early Miocene—Late Miocene	1

facies dominate the investigated carbonate successions (Tables 4 and 5). The heterozoan facies reach their maximum during the Burdigalian (Tables 4 and 5). Both type of calcifiers decrease through the time period as the non-skeletal grains dominated facies become more significant (Tables 4 and 5). The LBF-dominated facies display a clear peak during the Rupelian and reach their lowest abundance in the Aquitanian (Table 4). By taking together both LBF-dominated and LBF-codominated facies, the Rupelian peak can no longer be observed in both the formation-average and section-average representations, while the minimum during the Aquitanian still occurs (Table 5). Similarly, the abundance of CC dominated facies (either solely considering CC dominated facies or considering both CC dominated and CC codominated facies) displays a minimum during

TABLE 2 Percent distribution of the dominant components during the Palaeocene, Eocene, Oligocene, Miocene, following the section-average and the formation-average approaches, respectively.

Dominant components	LBF	LBF & RCA	LBF & GCA	LBF & CC	CC	CC & RCA	CC & EBF	RCA	RCA & Peloids	GCA	GCA & SBF	EBF	SBF	SBF & Peloid	Microbial crusts	Ooids	Peloids	Intraclasts	Mud	Heterozoan
Section-average (%)																				
Palaeocene	35.21	19.40	9.29	0.00	3.38	2.69	0.00	3.60	0.00	8.55	0.67	0.00	7.69	1.81	0.24	1.14	0.36	0.38	1.33	4.26
Eocene	78.21	3.21	0.28	0.00	0.61	0.00	0.00	0.95	0.03	0.33	0.11	2.39	4.97	0.00	0.38	0.25	0.07	0.00	2.95	5.35
Oligocene	47.93	17.91	0.00	4.40	1.80	8.51	0.00	2.06	0.00	0.00	0.00	0.00	2.86	0.00	0.00	0.29	1.51	0.00	7.81	5.06
Miocene	33.02	8.88	0.00	0.29	1.88	2.42	0.05	1.02	0.00	0.00	0.00	0.00	13.65	0.00	0.13	4.94	2.64	0.00	15.72	15.35
Formation-average (%)																				
Palaeocene	35.89	18.36	5.74	0.00	1.56	0.81	0.00	6.86	0.00	11.68	0.40	0.00	7.24	0.54	0.26	1.59	0.41	0.57	2.31	5.77
Eocene	77.26	3.65	0.71	0.00	0.51	0.00	0.00	1.81	0.08	0.83	0.29	2.54	6.53	0.00	0.13	0.21	0.02	0.00	2.04	3.38
Oligocene	41.34	11.90	0.00	32.71	0.99	2.90	0.00	1.57	0.00	0.00	0.00	0.00	2.82	0.00	0.00	0.05	0.29	0.00	3.19	2.23
Miocene	16.36	9.79	0.00	3.13	7.68	10.61	0.01	0.83	0.00	0.00	0.00	0.00	10.51	0.00	0.02	6.74	1.85	0.00	5.36	27.11

the Aquitanian (Tables 4 and 5). Both the facies dominated by non-skeletal grains in general and those characterised by intertidal muds specifically peak during the Aquitanian, in both the section-average and in the formation-average representations (Tables 4 and 5).

4.3 | Statistical analysis

The average abundances of the most relevant carbonate facies of the Palaeocene, Eocene, Oligocene and Miocene obtained from the various iterations of the bootstrap method show a normal distribution. Their confidence intervals (i.e. average ± 2 SD; Table 6) display limited to no overlap, especially with regards to the most volumetrically important facies: LBF-dominated, LBF codominated, RCA codominated and CC codominated facies (Figure 4). Sensitivity analysis also indicates that the calculated averages and standard deviations display no sensitivity to the number of the iterations of the bootstrap and very limited sensitivity to the size of the sub-sample. PERMANOVA dissimilarity analysis of the time slices indicates that these groups are dissimilar at $p < 0.05$.

5 | DISCUSSION

5.1 | Carbonate factories evolution

Large benthic foraminifera appear to be the most important carbonate producers within the investigated time interval in the southern Tethyan realm as they are very common in every region and in every epoch (Tables 2 and 3; Figures 3 and 5). They reach their maximum abundance during the Eocene (where they are overwhelmingly dominant) and their lowest during the Miocene (still remaining the most important carbonate producers). The results indicate that, from the late Palaeocene to the early Miocene, in the southern Tethyan realm, the majority share of the biogenic carbonates accumulated in shelfal carbonate factories, has been produced by benthic foraminifera. This now manifests with a large fraction of the shallow-water carbonates of the study area being comprised of LBF-dominated facies. These results are also supported by the lithostratigraphic information reported by Höntzsch et al. (2011) and Hussein (2019) for Egypt, by Schaub et al. (1995), Buchbinder et al. (2005) and Rosenfeld and Hirsch (2005) for Israel, by Farouk et al. (2013) for Jordan, by Alsharhan and Nairn (1995) for the Arabian Peninsula, by Sadooni and Alsharhan (2019) for UAE, by Bernecker (2014) for Oman, by Sissakian (2013), Ameen-Lawa and Ghafur (2015), and Sadooni and Alsharhan (2019) for

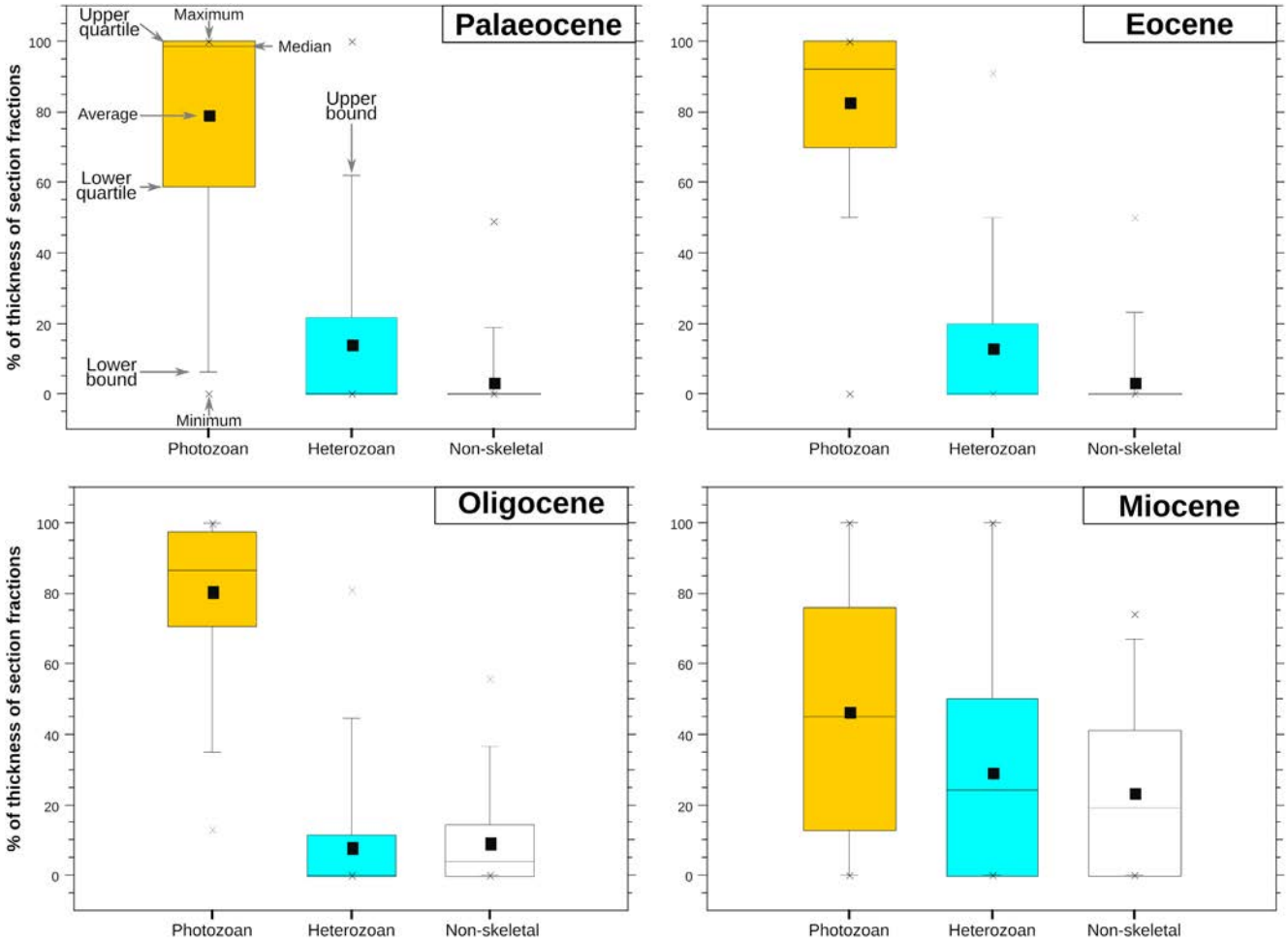

FIGURE 2 Box and whisker plots showing the Photozoan (yellow), Heterozoan (light blue) and non-skeletal dominated (white) facies distribution in the investigated fossil facies during the different epochs (Palaeocene, Eocene, Oligocene, Miocene).

Iraq, by Reuter et al. (2009), Van Buchem et al. (2010), Yazdi-Moghadam et al. (2018a), Hadi et al. (2019), Dill et al. (2020) and Benedetti et al. (2021) for Iran, by Akhtar and Butt (1999), Naveed and Chaudhry (2008), Afzal et al. (2011b), Özcan et al. (2015), Ahmad et al. (2016), Khan et al. (2018) and Özcan et al. (2018) for Pakistan, by Gaetani et al. (1983), Less et al. (2018) and Sarkar (2018) for India, and by Zhang et al. (2013) for China. Other reviews of Cenozoic carbonate production in the Eurasian province also highlighted a remarkable abundance of LBF during the Palaeocene, Eocene (where they dominates), Oligocene and early Miocene (BouDagher-Fadel, 2018; Cornacchia et al., 2021; Geel, 2000; Nebelsick et al., 2005; Pomar et al., 2017; Scheibner & Speijer, 2008). A similar pattern can be also observed in the American province (Aguilera et al., 2020).

In the modern oceans, LBF distribution is strongly controlled by temperature (Langer & Hottinger, 2000; Renema, 2018) and so is their diversity. Tropical assemblages display a much larger number of genera and species than sub-tropical ones (Beavington-Penney & Racey, 2004). During the early Eocene, following an extinction event at the Palaeocene–Eocene boundary, LBF became significantly more diverse with the rise of large nummulitids that would dominate LBF assemblages until the Bartonian (Benedetti & Papazzoni, 2022; BouDagher-Fadel, 2018). The high temperatures of the early Eocene as well as the temperature drop at the end of the Bartonian (Zachos et al., 2001) suggests, as already noted by other authors (Scheibner & Speijer, 2008), a strong relationship between temperature and LBF abundance. During the early Palaeogene their dominance started at low latitudes and progressed towards higher latitudes as temperatures rose, paralleled by a decrease of CC (Martín-Martín et al., 2020; Scheibner & Speijer, 2008). Therefore, LBF success during the Palaeogene would have been favoured by the greenhouse conditions that prevailed for most of the period (except during the Oligocene, when the opening of the Tasmanian and Drake passages lead to the isolation and the progressive build-up of ice on Antarctica; Zachos et al., 2001). Meta-analysis clearly shows that LBF facies

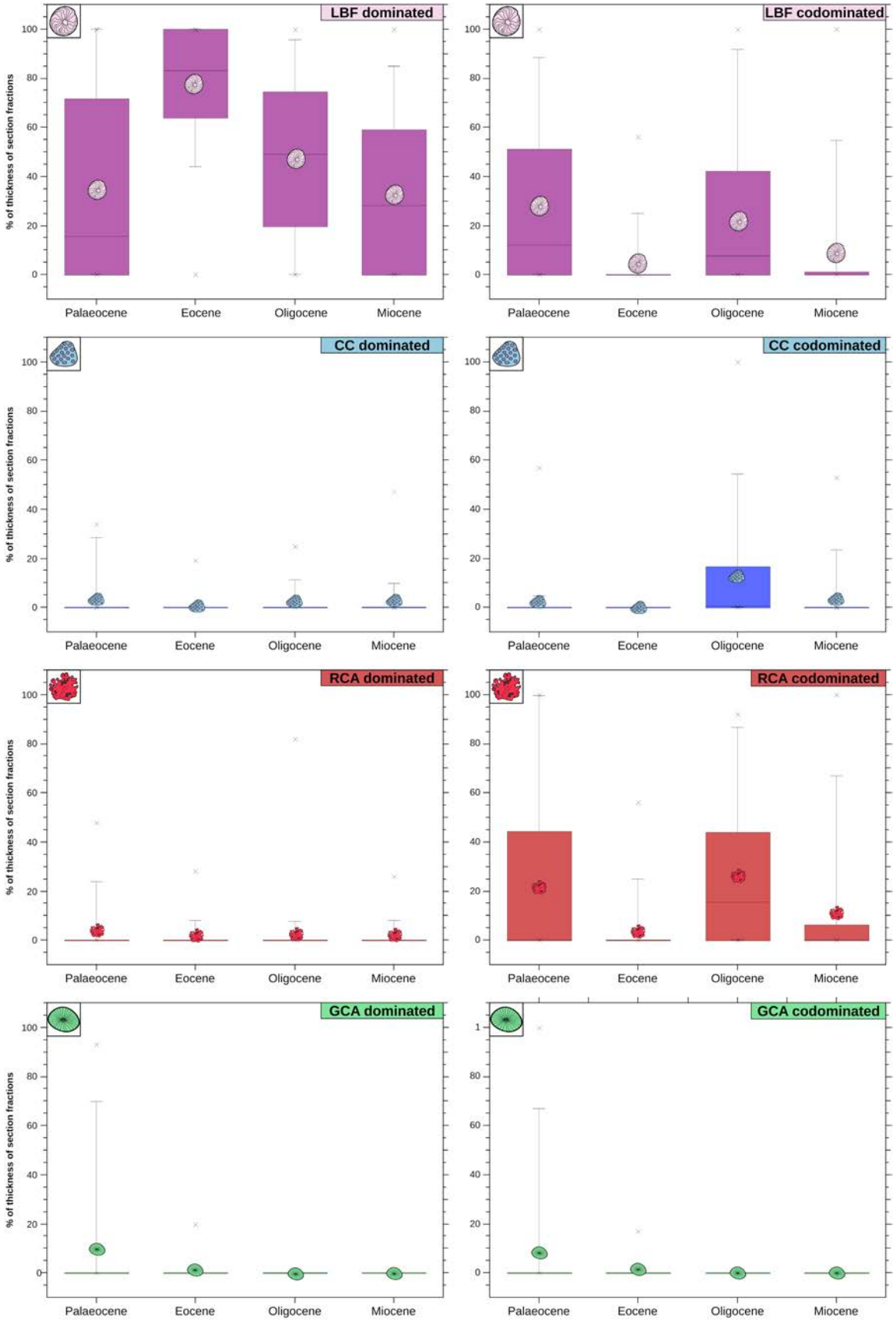

FIGURE 3 Box and whisker plots showing the distribution during time (Palaeocene, Eocene, Oligocene, Miocene) of the LBF-dominated and codominated facies (purple), CC dominated and codominated facies (blue), RCA dominated and codominated facies (red), and GCA dominated and codominated facies (green); the key for the statistical symbols of the box and whisker plot is as in Figure 2.

TABLE 3 Percent distribution of the main groups of carbonate grains (dominated plus codominated facies) during the Palaeocene, Eocene, Oligocene, Miocene, following the section-average and the formation-average approaches, respectively.

Dominated + Codominated facies	LBF	CC	RCA	GCA	EBF	Ooids and Peloids	Mud	Microbial crusts	Heterozoan
Section-average (%)									
Palaeocene	63.90	6.07	25.69	18.50	0.00	3.31	1.33	0.24	14.43
Eocene	81.70	0.61	4.20	0.72	2.39	0.34	2.95	0.38	10.43
Oligocene	70.24	14.71	28.49	0.00	0.00	1.80	7.81	0.00	7.91
Miocene	42.20	4.65	12.33	0.00	0.05	7.58	15.72	0.13	29.00
Formation-average (%)									
Palaeocene	60.00	2.36	26.03	17.82	0.00	2.54	2.31	0.26	13.95
Eocene	81.61	0.51	5.54	1.83	2.54	0.31	2.04	0.13	10.21
Oligocene	85.95	36.61	16.37	0.00	0.00	0.34	3.19	0.00	5.05
Miocene	29.27	21.42	21.22	0.00	0.01	8.59	5.36	0.02	37.63

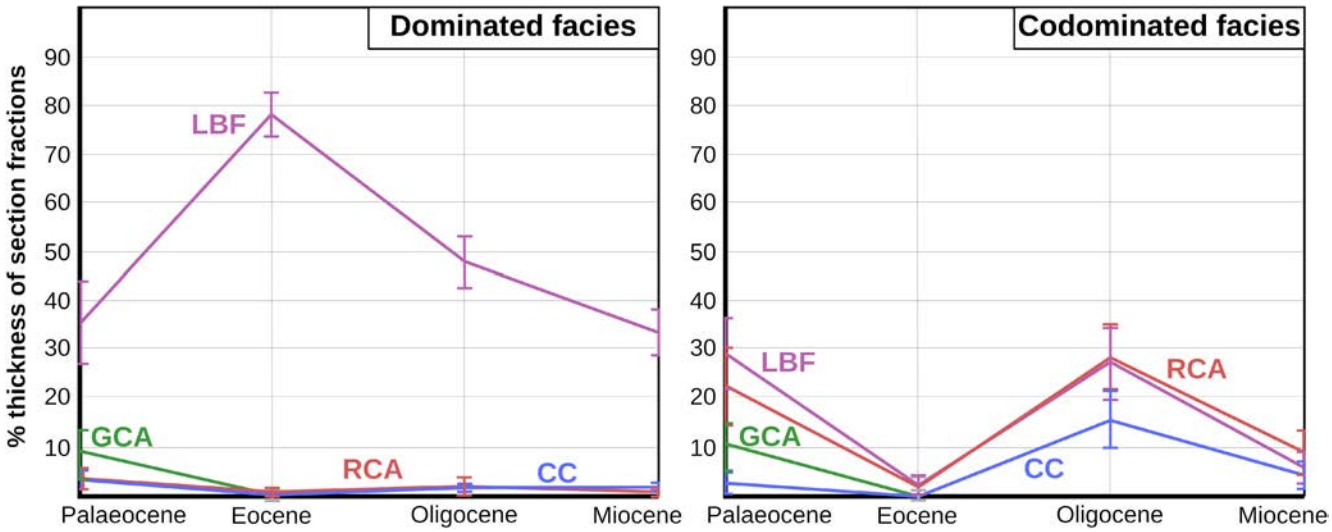

FIGURE 4 Bootstrap calculated averages (thick line) and confidence intervals (thin bars) of the most abundant and relevant carbonate factories in the study area during the Cenozoic; grey confidence intervals are related to less than zero minimum values of the confidence interval caused by the low average abundance of the facies during the epoch.

peak in the Eocene (which is mainly represented by the early Eocene in the database). However, taken together, LBF-dominated and codominated facies do not diminish much during the Oligocene. The review of Nebelsick et al. (2005), focussed on Eocene circum-Alpine carbonates, also indicates that LBF facies largely dominated during the middle Eocene, far after the Early Eocene Climatic Optimum. This suggests a more complex pattern. According to Pomar et al. (2017) and Hallock and Seddighi (2022), LBF are perfectly suited to deal with extreme oligotrophic conditions associated with periods of reduced thermohaline circulation. This might have played a role in fostering their abundance during the warm periods of the Palaeogene. The LBF also seem to be better adapted than CC to water turbidity related to nutrient abundance (Wilson & Vecsei, 2005), and to outperform both CC and RCA in environments characterised by high sedimentation rates (Coletti et al., 2021b; Lokier et al., 2009). It should be remembered that, although relatively complex, LBF are unicellular organisms, and thus, they are very flexible. Despite certain groups of LBF clearly evolving through geological time pursuing a K-strategy compared to other benthic foraminifera (see Hottinger, 1982), their life cycle is still significantly different from that of multicellular organism like RCA and CC. Furthermore, unlike CC and RCA, LBF are mobile and so they can relocate if they need to. The LBF probably took advantage of the reduced competition in shelfal settings caused by the harsh conditions created by the Palaeocene Eocene Thermal

TABLE 4 Percent distribution of the dominant components in the Oligocene (Rupelian, Chattian) and early Miocene (Aquitanian, Burdigalian), following the section-average and the formation-average approaches, respectively.

Dominant components	LBF	LBF & RCA	LBF & GCA	LBF & CC	CC	CC & RCA	CC & EBF	RCA	RCA & Peloids	GCA	GCA & SBF	EBF	SBF	SBF & Peloid	Microbial crusts	Ooids	Peloids	Intraclasts	Mud	Heterozoan
Section-average (%)																				
Rupelian	51.35	22.13	0.00	4.35	2.00	8.74	0.00	1.43	0.00	0.00	0.00	0.00	2.17	0.00	0.00	0.00	1.26	0.00	2.82	3.96
Chattian	45.50	15.95	0.00	4.73	1.82	8.98	0.00	2.52	0.00	0.00	0.00	0.00	3.41	0.00	0.00	0.45	1.75	0.00	10.84	4.05
Aquitanian	30.81	9.89	0.00	0.69	0.42	0.47	0.00	1.08	0.00	0.00	0.00	0.00	11.83	0.00	0.08	11.19	3.81	0.00	20.72	9.00
Burdigalian	37.61	6.95	0.00	0.00	2.45	1.03	0.11	0.87	0.00	0.00	0.00	0.00	16.61	0.00	0.18	0.45	0.84	0.00	13.32	19.61
Formation-average (%)																				
Rupelian	40.20	15.90	0.00	25.00	1.57	4.34	0.00	1.65	0.00	0.00	0.00	0.00	4.53	0.00	0.00	0.00	0.45	0.00	1.90	4.52
Chattian	35.28	14.97	0.00	34.67	1.28	4.02	0.00	2.42	0.00	0.00	0.00	0.00	0.83	0.00	0.00	0.10	0.38	0.00	4.41	1.65
Aquitanian	15.47	11.65	0.00	5.00	0.12	0.14	0.00	2.81	0.00	0.00	0.00	0.00	7.46	0.00	0.02	10.70	2.67	0.00	11.80	32.17
Burdigalian	24.83	14.41	0.00	0.00	7.56	0.73	0.04	1.35	0.00	0.00	0.00	0.00	14.31	0.00	0.06	0.71	1.11	0.00	7.71	27.19

Maximum and the other Palaeogene hyperthermals and, thanks to their adaptability, they thrived even after the end of the early Palaeogene greenhouse. The EBF, similarly to free-living LBF, reach peak abundance during the Eocene (Tables 3 and 4). Presently EBF are relatively rare and can produce centimetre-sized nodules (Bassi et al., 2012; Hottinger, 1983). However, during the early and middle Eocene LBF were a relevant group of reef-builders, creating extensive reefs in the Western Tethys (Perrin, 1992, 2009; Rasser, 1994). While modern EBF do not harbour symbionts (Leutenegger, 1984) and usually occur between water depths of 40 m and 105 m (Bassi et al., 2012; Rasser & Piller, 1997), Eocene EBF are often associated with shallow-water assemblages typical of the upper part of the photic zone (e.g. they are commonly associated with alveolinids) (Coletti et al., 2021b; Rasser, 1994; Tomás et al., 2016), indicating that Eocene EBF might have been relatively different from their modern counterparts. More detailed analysis might help clarify if Eocene EBF were symbiont bearing organisms or not, and thus suggest the environmental reasons for their abundance during the Eocene.

Colonial corals are abundant in the Palaeocene and in the Miocene, while they reach a peak during the Oligocene (Tables 2 and 3; Figures 3 and 5). They are rare during the Eocene (Tables 2 and 3; Figures 3 and 5). This is also supported by the lithostratigraphic information provided by Coletti et al. (2021a) for Cyprus, by Kuss and Boukhary (2008) for Egypt, by Whittle et al. (1995) and Sadooni and Alsharhan (2019) for UAE, by Bernecker (2014) for Oman, by Sissakian (2013), Ameen-Lawa and Ghafur (2015), Ghafur (2015) and Sadooni and Alsharhan (2019) for Iraq, by Reuter et al. (2009), Van Buchem et al. (2010), Ghaedi et al. (2016), Yazdi-Moghadam et al. (2018a, 2018b, 2021) and Dill et al. (2020) for Iran, by Afzal et al. (2011b) for Pakistan, by Less et al. (2018) and Sarkar (2018) for India. The results of this study are overall consistent with other reviews of Cenozoic CC distribution in the Eurasian province (Perrin & Bosellini, 2012; Pomar et al., 2017; Scheibner & Speijer, 2008), East Pacific province (López-Pérez, 2005, 2017) and American province (Budd, 2000; Johnson et al., 2008), that indicate the Oligocene as a favourable period for both CC and CC dominated reefs.

Similarly to LBF, this pattern seems to be strongly connected to global temperatures. In the Eurasian province, during the Palaeocene, CC are actually more abundant during the early to late Palaeocene interval (Martín-Martín et al., 2020; Scheibner & Speijer, 2008). This time interval is characterised by temperatures lower than those of the latest Palaeocene and of the early Eocene (Barnet et al., 2019). During the early to middle Eocene CC are relatively rare and only become relevant carbonate producers

TABLE 5 Percent distribution of the main groups of carbonate grains (dominated plus codominated facies) in the Oligocene (Rupelian, Chattian) and early Miocene (Aquitanian, Burdigalian), following the section-average and the formation-average approaches, respectively.

Dominated + Codominated facies	LBF	CC	RCA	GCA	EBF	Ooids and Peloids	Mud	Microbial crusts	Heterozoan
Section-average (%)									
Rupelian	77.83	15.09	32.30	0.00	0.00	1.26	2.82	0.00	6.13
Chattian	66.18	15.52	27.45	0.00	0.00	2.20	10.84	0.00	7.45
Aquitanian	41.39	1.58	11.44	0.00	0.00	15.00	20.72	0.08	20.83
Burdigalian	44.55	3.58	8.84	0.00	0.11	1.29	13.32	0.18	36.21
Formation-average (%)									
Rupelian	81.10	30.91	21.89	0.00	0.00	0.45	1.90	0.00	9.05
Chattian	84.92	39.97	21.41	0.00	0.00	0.48	4.41	0.00	2.48
Aquitanian	32.12	5.26	14.59	0.00	0.00	13.36	11.80	0.02	39.63
Burdigalian	39.24	8.33	16.49	0.00	0.04	1.81	7.71	0.06	41.49

again during the late Eocene (Bernecker, 2014; Nebelsick et al., 2005; Scheibner & Speijer, 2008), which is the coldest stage of the epoch (Zachos et al., 2001). The Oligocene is the coldest period of the Palaeogene (Zachos et al., 2001), and it is recognised worldwide as a period of great abundance of CC (Dishon et al., 2020). During the early Miocene CC are still very common, but during the middle Miocene, worldwide, RCA become significantly more abundant in shelfal tropical situations at the expenses of CC (Bialik et al., 2022; Cornacchia et al., 2021; Esteban, 1979, 1996; Halfar & Mutti, 2005; López-Pérez, 2005). The abundance of CC increased during the late Miocene in the Western Tethys (Cornacchia et al., 2021; Esteban, 1979, 1996; Pomar et al., 2017; Pomar & Hallock, 2007) and during the Plio-Pleistocene in the East Pacific and in the Caribbean (Johnson et al., 2008; López-Pérez, 2005). Thus, the distribution of CC during the Neogene can be also related to temperatures as CC are less abundant in the warm Middle Miocene Climatic Optimum and more abundant during cooler periods (Dishon et al., 2020; Herbert et al., 2016; Steinthorsdottir et al., 2020; Zachos et al., 2001). The CC presently thrive in a narrow temperature range and are severely damaged (i.e. the coral bleaching) whenever temperatures exceed this threshold (Crabbe, 2008; Marshall & Clode, 2004), it is conceivable that the warm peaks of the Cenozoic might have had a detrimental effect on CC abundance. Colder periods are also characterised by a stronger oceanic circulation than warmer periods, and this factor could also have favoured CC over other carbonate producers like LBF (Pomar et al., 2017). Furthermore, colder periods are favourable towards aragonite-producing organisms like CC (Hallock, 1997; Scheibner & Speijer, 2008), whereas the ocean chemistry of warm periods (like the Palaeocene–Eocene) is favourable for calcite generation (Stanley, 2006) and possibly detrimental to CC. However, the low pH (Boudreau et al., 2019), which characterised most of the Palaeocene and Eocene, likely had a significant negative impact also on the accumulation and preservation potential of CC—if they even calcified in shallow water at this time and had not shifted to a non-calcifying lifestyle (Fine & Tchernov, 2007). With the currently available data, disentangling the effects of these factors is probably impossible, although it is clear that temperature played an important role.

The RCA abundance displays a pattern similar to the one of CC and characterised by a minimum during the Eocene (Tables 2 and 3; Figures 3 and 5). This is supported by the lithostratigraphic information provided by Coletti et al. (2021a) for Cyprus, by Kuss and Boukhary (2008) for Egypt, by Whittle et al. (1995) for UAE, by Afzal et al. (2011b) for Pakistan, by Bernecker (2014) for Oman, by Seyrafian and Toraby (2005), Reuter et al. (2009), Ghaedi et al. (2016) and Yazdi-Moghadam et al. (2021) for Iran. Within the various sections the abundance of CC and RCA codominant facies shows a positive correlation in the Palaeocene and in the Miocene, but not as clearly during the Eocene and the Oligocene (Figure 3).

Modern RCA are extremely adaptable and can thrive in both warm and cold climates, in both oligotrophic and nutrient-rich water and from the shallow intertidal zone to the lowest limit of the photic zone (Pomar et al., 2017; Riosmena-Rodríguez, 2017). The CC require a hard substrate for their initial recruitment on the seafloor and RCA can generate hard substrates. Free-living nodules can progressively coalesce leading to the creation of a hard substrate suitable for the colonisation of other organisms or the expansion of RCA bioconstructions. In turn the complex framework of CC-reefs creates several niches that can be used by coralline algae. Therefore, to a certain extent, the two groups are mutually beneficial to one another, justifying why the periods favourable for the former can be also favourable for the latter. However, most of the analysed papers pay little

TABLE 6 Bootstrap analysis of the averages of the most abundant and relevant Cenozoic carbonate factories of the study area; the analysis was performed using a 2/3 sub-sample size and 10,000 iterations.

Dominated facies	Palaeocene	Eocene	Oligocene	Miocene	Codominated facies	Palaeocene	Eocene	Oligocene	Miocene
LBF mean (%)	**35.19**	**78.20**	**47.86**	**33.03**	LBF mean (%)	**28.70**	**2.27**	**26.97**	**5.82**
LBF standard deviation (%)	**4.36**	**2.24**	**2.66**	**2.35**	LBF standard deviation (%)	**3.62**	**1.00**	**3.57**	**1.60**
LBF lower confidence interval (%)	26.47	73.72	42.54	28.33	LBF lower confidence interval (%)	21.46	0.27	19.83	2.62
LBF upper confidence interval (%)	43.91	82.68	53.18	37.73	LBF upper confidence interval (%)	35.94	4.27	34.11	9.02
CC mean (%)	**3.39**	**0.31**	**1.78**	**1.88**	CC mean (%)	**2.70**	**0.00**	**15.55**	**4.31**
CC (standard deviation) (%)	**0.94**	**0.60**	**0.40**	**0.52**	CC (standard deviation) (%)	**1.27**	**0.00**	**2.77**	**1.39**
CC lower confidence interval (%)	1.51	−0.89	0.98	0.84	CC lower confidence interval (%)	0.16	0.00	10.01	1.53
CC upper confidence interval (%)	5.27	1.51	2.58	2.92	CC upper confidence interval (%)	5.24	0.00	21.09	7.09
RCA mean (%)	**3.61**	**0.95**	**2.05**	**1.02**	RCA mean (%)	**22.17**	**1.91**	**27.87**	**8.95**
RCA standard deviation (%)	**1.07**	**0.39**	**0.91**	**0.33**	RCA standard deviation (%)	**3.83**	**1.00**	**3.35**	**2.27**
RCA lower confidence interval (%)	1.47	0.17	0.23	0.36	RCA lower confidence interval (%)	14.51	−0.09	21.17	4.41
RCA upper confidence interval (%)	5.75	1.73	3.87	1.68	RCA upper confidence interval (%)	29.83	3.91	34.57	13.49
GCA mean (%)	**8.50**	**0.33**	**0.00**	**0.00**	GCA mean (%)	**9.90**	**0.57**	**0.00**	**0.00**
GCA standard deviation (%)	**2.53**	**0.24**	**0.00**	**0.00**	GCA standard deviation (%)	**2.53**	**0.31**	**0.00**	**0.00**
GCA lower confidence interval (%)	3.44	−0.15	0.00	0.00	GCA lower confidence interval (%)	4.84	−0.05	0.00	0.00
GCA upper confidence interval (%)	13.56	0.81	0.00	0.00	GCA upper confidence interval (%)	14.96	1.19	0.00	0.00

Mean values and standard deviation values are indicated in bold.

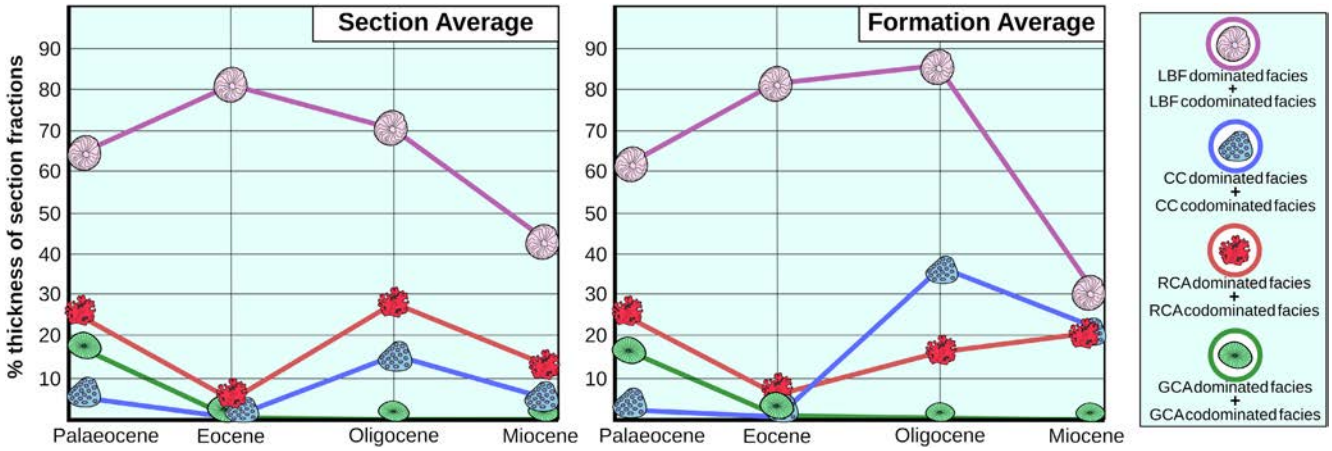

FIGURE 5 Summary diagrams showing the distribution of the main recognised facies (LBF, CC, RCA, GCA) during the Palaeocene, the Eocene, the Oligocene, and the Miocene, using the two different approaches (see Methods): The section-average and the formation-average approaches. Note the preponderance of LBF-dominated and codominated facies in all the epochs; the key to the symbols of the various carbonate producers is as in Figure 3; colour coding is as in Figure 4; as certain facies can be codominated by, for example LBF and CC (and thus be included in both the CC dominated + CC codominated facies and in the LBF-dominated + LBF codominated facies), in this graph the total can exceed 100%.

attention to RCA in comparison to LBF (which are useful for biostratigraphy), and CC (that can be easily observed in the outcrops), therefore a bias in the database that could lead to an underestimation of RCA can not be excluded.

Within the study area, during the Palaeocene, GCA are rarely a dominant component of the skeletal assemblage (Tables 2 and 3; Figures 3 and 5). In the Eocene, they dominate very rarely, while in the Oligocene and in the Miocene they occur only as a minor component of the skeletal assemblage. These results are supported by the lithostratigraphic information provided by Höntzsch et al. (2011) for Egypt, by Nafarieh et al. (2019) and Benedetti et al. (2021) for Iran, by Akhtar and Butt (1999), Afzal et al. (2011b), Khan et al. (2018) and Khitab et al. (2020) for Pakistan, by Gaetani et al. (1983) for India, and by Zhang et al. (2013) for China. Unlike the results given here, the review of Pomar et al. (2017) of Cenozoic carbonates of western-central Tethys indicates abundant GCA only in the Danian (mainly dasyclads) and in the Miocene (mainly Halimedales). Based on the fossil record, during the Cenozoic, GCA biodiversity peaks in the Palaeocene and decreases afterwards (Aguirre & Riding, 2005). This pattern is consistent with the abundance of GCA in the successions of the study area. However, while biodiversity may be related to abundance it is usually decoupled from carbonate production (Johnson et al., 2008). Modern GCA mostly precipitate aragonite and are thus easily susceptible to diagenetic dissolution, which can start even when the algae are still alive (Granier, 2012). Several fossil taxa of Dasycladales are thought to have precipitated calcite instead of aragonite (Granier, 2012). The last of these supposedly calcitic taxa occurred during the Eocene (Granier, 2012). Therefore, the observed pattern of GCA distribution might be, possibly similar to CC, related to a preservation bias as opposed to an environmental variable as in the case of LBF. The progressive decrease of GCA abundance throughout the Cenozoic in this region might have been connected to a transition from early Palaeogene assemblages rich in calcite-producing taxa to Neogene assemblages entirely constituted of aragonitic taxa.

5.2 | Regional and global implications

Several remarkable similarities can be observed by comparing these results for South-western and Western Central Asia with the other few available reviews of carbonate production: the peak in LBF abundance during the Eocene and the increase in coral abundance during the Oligocene (Aguilera et al., 2020; Johnson et al., 2008; Kiessling et al., 1999; Nebelsick et al., 2005; Pomar et al., 2017; Scheibner & Speijer, 2008). These changes are likely to have been strongly related to temperature, as the global increase in both CC diversity and importance as carbonate producers is paired with a decrease in temperatures, while the Eocene widespread abundance of LBF is heralded by high global temperatures (Zachos et al., 2001). The CC achieve the highest calcification rates within a narrow temperature range (Crabbe, 2008; Marshall & Clode, 2004). This range is usually much larger for LBF (Titelboim et al., 2019), suggesting that LBF can take advantage of the detrimental effect that very high temperatures have on their competitors. These results are backed by quantitative data on facies abundance, and

thus provide a strong argument in favour of the major rearrangements of shallow-water carbonate factories at the Palaeocene–Eocene and Eocene–Oligocene boundaries indicated by the other reviews. As these changes are witnessed at the global scale and are most likely temperature driven, they provide clear evidence on the long term effect of temperatures on carbonate factories and shelfal biomes.

Unlike the north-western Mediterranean Tethys area analysed by Pomar and Hallock (2007) and Pomar et al. (2004, 2012, 2017), LBF are always the dominant carbonate producers, even after the Eocene. The LBF, in north-western Mediterranean Tethys, are reported to diminish during the Oligocene and show a resurgence during the Miocene (Pomar et al., 2017). This is not observed in the study area. Such a difference could be still, at least partially, temperature related, as the study area was located south of the north-western Mediterranean Tethys and thus was probably more favourable for LBF. During the Oligocene and the early Miocene, thanks to global cooling and a progressive northward shift, southern Tethys became more favourable to CC, leading to their increase. This cooling is also evidenced by the progressive increase of Heterozoan carbonate facies (Figure 2). While in the north-western Mediterranean Tethys RCA abundance increases only in the Miocene, in the study area, RCA facies are already very common by the Oligocene following the increase in CC, suggesting a favourable relationship with the two groups.

The abundance of non-skeletal facies related to restricted conditions (Flügel, 2004) peaks in the early Miocene and in particular in the Aquitanian. This is also supported by the lithostratigraphic information provided by Al-Juboury and McCann (2008) and Ameen-Lawa and Ghafur (2015) for Iraq, Reuter et al. (2009) and Mohammadi et al. (2013) for Iran. During the Miocene, the convergence between the African-Arabian and Eurasian plate lead to the progressive restriction and then to the closure of the Mediterranean–Indian Ocean Seaway (Robertson et al., 2012; Rögl, 1999). Sedimentation rates in the Eastern Mediterranean indicates that most of the deep water restriction occurred in the 24–21 Ma interval (Torfstein & Steinberg, 2020), while Nd isotopes indicates that surface water exchange was reduced by *ca* 90% at *ca* 20 Ma (Bialik et al., 2019). Consequently, although a shallow connection between the two basins persisted for much longer (Buchbinder, 1996; Cornacchia et al., 2018; Sissakian, 2013), most of the restriction occurred during the Aquitanian, consistent with the observed peak of carbonate facies related to restricted marine conditions.

Bootstrap analysis and the comparison of formation-averages and section-averages indicate that the observed trends displayed by the most relevant carbonate facies, that account for most of the thickness of the analysed carbonate successions and for most of the variability of the system, can not be simply considered a result of the noise of the dataset. Whether different sub-samples are considered, (i.e., the carbonate successions analysed), whether or not the results are grouped based on their geological provenance, the same general trends pop out (Figures 4 and 5). The remarkable differences between the different time slices, highlighted by dissimilarity analysis, also testifies in favour of the robustness of the results as a randomised development process of the various carbonate factories would have ended up with similar abundances of the various carbonate facies in each epoch. While the formation-average/section-average approach and the bootstrap suggest that the bias related to the geographical position of the studied sections has only a limited effect, the accuracy and the reliability of the source material, which most times consists of qualitative descriptions, prevents more detailed analysis. To test the effects of the relative position of the various sections within the study area, which in turn affects temperature and nutrient availability, a proper quantification of the various components of the skeletal assemblages would be necessary. Such an analysis would also require further subdivision of the database, leading to unequal distribution of sections in the various time slices and their uneven geographical distribution, reducing the robustness of the results as the new sub-sets would be probably characterised by widely different sample-sizes.

6 | CONCLUSIONS

This meta-analysis of Palaeocene to Miocene outcrops of shallow carbonates of the South-western and Western Central Asian regions highlighted several trends in the composition of carbonate factories and in the abundance of carbonate-producing organisms. Large benthic foraminifera are the most quantitatively relevant group of carbonate producers during the whole investigated period, with their abundance peaking during the Eocene and dwindling only during the Miocene. The abundance of CC is highest during the Oligocene and lowest during the Eocene (which in the database is mainly represented by the lower Eocene). Both patterns seem to be related to global temperatures which (within the investigated time period) reach their maximum during the early Eocene and their lowest in the Oligocene. Colonial corals achieve the highest calcification rate in a very narrow temperature range compared to large benthic foraminifera. The very high temperatures of the early Palaeogene of the tropical southern Tethys, might, thus, have favoured LBF-dominated carbonate factories. Thanks to their adaptability LBF would have kept their position as dominant carbonate producers for the whole period, even after the end of the early Palaeogene greenhouse. Red calcareous algae display a pattern much like the one of CC. Since RCA and CC are currently the

main framework builder of shallow-water tropical reefs it is possible that, on the large scale, the two groups are probably mutually beneficial to one another in terms of carbonate production. Green calcareous algae decreased from the Palaeocene onward. As the last taxa of presumably calcitic GCA went extinct during the Eocene, it is possible that their overall decrease as carbonate producers might be related to a preservation bias connected to the transition towards modern assemblages that are entirely constituted by fragile, aragonite-producing, taxa.

Nutrient abundance and seawater chemistry most likely also played a role in shaping these large-scale patterns of carbonate production. However, any attempt at disentangling the weight of the various variables not backed by more accurate and standardised data on the skeletal assemblages, would be only speculative.

The Aquitanian peak in the abundance of carbonate facies related to very shallow and/or restricted marine conditions is most likely connected to the progressive narrowing of the Tethys Ocean related to the ongoing collision with the Arabian plate.

Overall, this meta-analysis displays a clear agreement between large-scale patterns in shallow-water carbonate sedimentation and both environmental and geological processes, indicating the trove of information locked within the shallow-water sedimentary record. However, to unlock this potential, a standardised, quantitative and reproducible approach is absolutely necessary.

ACKNOWLEDGEMENTS

The authors are grateful to Professor Sam Purkis for his revisions and his wise suggestions that have significantly improved the manuscript, and to the editorial board and editorial office of The Depositional Record for their help and their courtesy. G.C., L.M. and G.B. would like to thank Milano Bicocca University for funding their doctoral and post-doctoral grants. O.M.B. is supported by the Marie Skłodowska Curie fellowship (101003394-RhodoMalta). The first and last authors would also like to thank the IAS for supporting their research activities and for creating an environment conducive to the development of this study. This research represents a scientific contribution of Project MIUR—Dipartimenti di Eccellenza 2018-2022.

DATA AVAILABILITY STATEMENT

The data that support the findings of this study are openly available at https://doi.org/10.6084/m9.figshare.19323821.v1

ORCID

Giovanni Coletti https://orcid.org/0000-0002-0454-0413
Or M. Bialik https://orcid.org/0000-0003-1915-7297

REFERENCES

Adabi, M.H., Kakemem, U. & Sadeghi, A. (2016) Sedimentary facies, depositional environment, and sequence stratigraphy of Oligocene–Miocene shallow water carbonate from the Rig Mountain, Zagros basin (SW Iran). *Carbonates and Evaporites*, *31*(1), 69–85.

Adabi, M.H., Zohdi, A., Ghabeishavi, A. & Amiri-Bakhtiyar, H. (2008) Applications of nummulitids and other larger benthic foraminifera in depositional environment and sequence stratigraphy: an example from the Eocene deposits in Zagros Basin, SW Iran. *Facies*, *54*(4), 499–512.

Afzal, J., Williams, M. & Aldridge, R.J. (2009) Revised stratigraphy of the lower Cenozoic succession of the greater Indus Basin in Pakistan. *Journal of Micropalaeontology*, *28*(1), 7–23.

Afzal, J., Williams, M., Leng, M.J. & Aldridge, R.J. (2011a) Dynamic response of the shallow marine benthic ecosystem to regional and pan-Tethyan environmental change at the Paleocene–Eocene boundary. *Palaeogeography, Palaeoclimatology, Palaeoecology*, *309*(3–4), 141–160.

Afzal, J., Williams, M., Leng, M.J., Aldridge, R.J. & Stephenson, M.H. (2011b) Evolution of Paleocene to early Eocene larger benthic foraminifer assemblages of the Indus Basin, Pakistan. *Lethaia*, *44*(3), 299–320.

Agard, P., Omrani, J., Jolivet, L., Whitechurch, H., Vrielynck, B., Spakman, W., Monié, P., Meyer, B. & Wortel, R. (2011) Zagros orogeny: a subduction-dominated process. *Geological Magazine*, *148*(5–6), 692–725.

Aguilera, O., Bencomo, K., de Araújo, O.M.O., Dias, B.B., Coletti, G., Lima, D., Silane, A.F., Polk, M., Alves-Martin, M.V., Jaramillo, C., Kutter, V.T. & Lopes, R.T. (2020) Miocene heterozoan carbonate systems from the western Atlantic equatorial margin in South America: the Pirabas formation. *Sedimentary Geology*, *407*, 1–28. https://doi.org/10.1016/j.sedgeo.2020.105739

Aguirre, J. & Riding, R. (2005) Dasycladalean algal biodiversity compared with global variations in temperature and sea level over the past 350 Myr. *Palaios*, *20*(6), 581–588.

Ahmad, S., Kroon, D., Rigby, S. & Khan, S. (2016) Paleogene Nummulitid biostratigraphy of the Kohat and Potwar basins in North-Western Pakistan with implications for the timing of the closure of eastern Tethys and uplift of the western Himalayas. *Stratigraphy*, *13*, 277–301.

Ahmad, S., Wadood, B., Khan, S., Ullah, A., Mustafa, G., Hanif, M. & Ullah, H. (2020) The sedimentological and stratigraphical analysis of the Paleocene to early Eocene Dungan formation, Kirthar fold and Thrust Belt, Pakistan: implications for reservoir potential. *Journal of Sedimentary Environments*, *5*(4), 473–492.

Akhtar, M. & Butt, A.A. (1999) Microfacies and foraminiferal assemblages from the early tertiary rocks of the kala Chitta range (northern Pakistan). *Géologie Méditerranéenne*, *26*(3), 185–201.

Al-Juboury, A.I. & McCann, T. (2008) The middle Miocene Fatha (lower Fars) formation, Iraq. *GeoArabia*, *13*(3), 141–174.

Al-Kahtany, K.M. (2017) Facies development of the Middle Miocene reefal limestone in Northwest Saudi Arabia. *Journal of African Earth Sciences*, *130*, 134–140.

Al-Qayim, B., Ibrahim, A. & Kharajiany, S. (2016) Microfacies and sequence stratigraphy of the Oligocene–Miocene sequence at

Golan Mountain, Kurdistan, Iraq. *Carbonates and Evaporites*, *31*(3), 259–276.

Alsharhan, A.S. & Nairn, A.E.M. (1995) Tertiary of the Arabian Gulf: sedimentology and hydrocarbon potential. *Palaeogeography, Palaeoclimatology, Palaeoecology*, *114*(2–4), 369–384.

Ameen-Lawa, F.A. & Ghafur, A.A. (2015) Sequence stratigraphy and biostratigraphy of the prolific late Eocene, Oligocene and early Miocene carbonates from Zagros fold-thrust belt in Kurdistan region. *Arabian Journal of Geosciences*, *8*(10), 8143–8174.

Amirshahkarami, M. (2013) Microfacies correlation analysis of the Oligocene-Miocene Asmari Formation, in the central part of the Rag-e-Safid anticlinal oil field, Zagros Basin, south-West Iran. *Turkish Journal of Earth Sciences*, *22*(2), 204–219.

Amirshahkarami, M. & Karavan, M. (2015) Microfacies models and sequence stratigraphic architecture of the Oligocene–Miocene Qom Formation, south of Qom City, Iran. *Geoscience Frontiers*, *6*(4), 593–604.

Amirshahkarami, M., Vaziri-Moghaddam, H. & Taheri, A. (2007a) Paleoenvironmental model and sequence stratigraphy of the Asmari Formation in Southwest Iran. *Historical Biology*, *19*(2), 173–183.

Amirshahkarami, M., Vaziri-Moghaddam, H. & Taheri, A. (2007b) Sedimentary facies and sequence stratigraphy of the Asmari formation at chaman-Bolbol, Zagros Basin, Iran. *Journal of Asian Earth Sciences*, *29*(5–6), 947–959.

Amirshahkarami, M. & Zebarjadi, E. (2018) Late Paleocene to early Eocene larger benthic foraminifera biozones and microfacies in Estahbanate area, southwest of Iran with Thetyan biozones correlation. *Carbonates and Evaporites*, *33*(4), 869–884.

An, W., Hu, X., Garzanti, E., Wang, J.G. & Liu, Q. (2021) New precise dating of the India-Asia collision in the Tibetan Himalaya at 61 Ma. *Geophysical Research Letters*, *48*(3), e2020GL090641.

Avarjani, S., Mahboubi, A., Moussavi-Harami, R., Amiri-Bakhtiar, H. & Brenner, R.L. (2015) Facies, depositional sequences, and biostratigraphy of the oligo-Miocene Asmari Formation in Marun oilfield, North Dezful embayment, Zagros Basin, SW Iran. *Palaeoworld*, *24*(3), 336–358.

Avni, Y., Segev, A. & Ginat, H. (2012) Oligocene regional denudation of the northern Afar dome: pre-and syn-breakup stages of the Afro-Arabian plate. *Bulletin*, *124*(11–12), 1871–1897.

Babazadeh, S.A. & Alavi, M. (2013) Paleoenvironmental model for early Eocene larger benthic foraminiferal deposits from South Birjand region, East Iran. *Revue de Paléobiologie, Genève*, *32*(1), 223–233.

Bagherpour, B. & Vaziri, M.R. (2012) Facies, paleoenvironment, carbonate platform and facies changes across Paleocene Eocene of the Taleh Zang formation in the Zagros Basin, SW-Iran. *Historical Biology*, *24*(2), 121–142.

Ballato, P., Mulch, A., Landgraf, A., Strecker, M.R., Dalconi, M.C., Friedrich, A. & Tabatabaei, S.H. (2010) Middle to late Miocene Middle Eastern climate from stable oxygen and carbon isotope data, southern Alborz mountains, N Iran. *Earth and Planetary Science Letters*, *300*(1–2), 125–138.

Banerjee, S., Khanolkar, S. & Saraswati, P.K. (2018) Facies and depositional settings of the middle Eocene-Oligocene carbonates in Kutch. *Geodinamica Acta*, *30*(1), 119–136.

Barnet, J.S., Littler, K., Westerhold, T., Kroon, D., Leng, M.J., Bailey, I., Röhl, U. & Zachos, J.C. (2019) A high-Fidelity benthic stable isotope record of late cretaceous–early Eocene climate change and carbon-cycling. *Paleoceanography and Paleoclimatology*, *34*(4), 672–691.

Bassi, D., Iryu, Y., Humblet, M., Matsuda, H., Machiyama, H., Sasaki, K., Matsuda, S., Arai, K. & Inoue, T. (2012) Recent macroids on the Kikai jima shelf, Central Ryukyu Islands, Japan. *Sedimentology*, *59*, 2024–2041.

Basso, D., Coletti, G., Bracchi, V.A. & Yazdi-Moghadam, M. (2019) Lower oligocene coralline algae of the Uromieh section (Qom formation, NW Iran) and the oldest record of *Titanoderma pustulatum* (Corallinophycidae, Rhodophyta). *Rivista Italiana di Paleontologia e Stratigrafia*, *125*(1), 197–218.

Beavington-Penney, S.J. & Racey, A. (2004) Ecology of extant nummulitids and other larger benthic foraminifera: applications in palaeoenvironmental analysis. *Earth-Science Reviews*, *67*(3–4), 219–265.

Beavington-Penney, S.J., Wright, V.P. & Racey, A. (2006) The middle Eocene Seeb formation of Oman: an investigation of acyclicity, stratigraphic completeness, and accumulation rates in shallow marine carbonate settings. *Journal of Sedimentary Research*, *76*(10), 1137–1161.

Benedetti, A., Consorti, L., Schlagintweit, F. & Rashidi, K. (2021) *Ornatorotalia* pila n. sp. from the late Palaeocene of Iran: ecological, evolutionary and paleobiogeographic inferences. *Historical Biology*, *33*(9), 1796–1803.

Benedetti, A. & Papazzoni, A. (2022) Rise and fall of rotaliid foraminifera across the Paleocene and Eocene times. *Micropaleontology*, *68*, 185–196.

Bernecker, M. (2014) Palaeogene carbonates of Oman: lithofacies and stratigraphy. In: Rocha, R., Pais, J., Kullberg, J. & Finney, S., (Eds.) *STRATI 2013*. Cham: Springer, pp. 71–74.

Bialik, O.M., Frank, M., Betzler, C., Zammit, R. & Waldmann, N.D. (2019) Two-step closure of the Miocene Indian Ocean gateway to the Mediterranean. *Scientific Reports*, *9*(1), 1–10.

Bialik, O.M., Jarochowska, E. & Grossowicz, M. (2021) Ordination analysis in sedimentology, geochemistry and palaeoenvironment—background, current trends and recommendations. *The Depositional Record*, *7*, 541–563.

Bialik, O.M., Reolid, J., Kulhanek, D.K., Hincke, C., Waldmann, N.D. & Betzler, C. (2022) Sedimentary response to current and nutrient regime rearrangement in the Eastern Mediterranean during the early to middle Miocene (Southwestern Cyprus). *Palaeogeography, Palaeoclimatology, Palaeoecology*, *588*, 110819.

Blondeau, A., Bassoulet, J.P., Colchen, M., Han, T.L., Marcoux, J., Mascle, G. & Van Haver, T. (1986) Disparition des formations marines à l'Éocène inférieur en Hymalaia. *Sciences de la Terre, Memorire*, *47*, 103–111.

Bosellini, F. & Perrin, C. (2008) Estimating Mediterranean Oligocene-Miocene Sea surface temperatures: an approach based on coral taxonomic richness. *Palaeogeography Palaeoclimatology Palaeoecology*, *258*, 71–88.

BouDagher-Fadel, M.K. (2018) *Evolution and geological significance of larger benthic foraminifera*. London: University College London Press, p. 693.

Boudreau, B.P., Middelburg, J.J., Sluijs, A. & van der Ploeg, R. (2019) Secular variations in the carbonate chemistry of the oceans over the Cenozoic. *Earth and Planetary Science Letters*, *512*, 194–206.

Buchbinder, B. (1996) Miocene carbonates of the eastern Mediterranean, the Red Sea and the Mesopotamian Basin: geodynamic and eustatic controls. In: Franseen, E.K., Esteban, M., Ward, W.C., & Rouchy, J.M. (Eds.) *Models for carbonate*

stratigraphy, from Miocene reef complex of the Mediterranean area. Concepts in Sedimentology and Paleontology 5. Tulsa, OK: Society for Sedimentary Geology, pp. 89–96.

Buchbinder, B., Calvo, R. & Siman-Tov, R. (2005) The Oligocene in Israel: a marine realm with intermittent denudation accompanied by mass-flow deposition. *Israel Journal of Earth Sciences*, *54*(2), 63–85.

Budd, A.F. (2000) Diversity and extinction in the Cenozoic history of Caribbean reefs. *Coral Reefs*, *19*(1), 25–35.

Coletti, G., Balmer, E.M., Bialik, O.M., Cannings, T., Kroon, D., Robertson, A.H.F. & Basso, D. (2021a) Microfacies evidence for the evolution of Miocene coral-reef environments in Cyprus. *Palaeogeography Palaeoclimatology Palaeoecology*, *584*, 11067.

Coletti, G., Basso, D., Betzler, C., Robertson, A.H., Bosio, G., El Kateb, A., Foubert, A., Meilijson, A. & Spezzaferri, S. (2019) Environmental evolution and geological significance of the Miocene carbonates of the Eratosthenes Seamount (ODP Leg 160). *Palaeogeography, Palaeoclimatology, Palaeoecology*, *530*, 217–235.

Coletti, G., Basso, D. & Frixa, A. (2017) Economic importance of coralline carbonates. In: *Rhodolith/Maërl beds: a global perspective*. Cham: Springer, pp. 87–101.

Coletti, G., Mariani, L., Garzanti, E., Consani, S., Bosio, G., Vezzoli, G., Xiumian, H. & Basso, D. (2021b) Skeletal assemblages and terrigenous input in the Eocene carbonate systems of the Nummulitic limestone (NW Europe). *Sedimentary Geology*, *425*, 106005.

Corlett, H.J., Bastesen, E., Gawthorpe, R.L., Hirani, J., Hodgetts, D., Hollis, C. & Rotevatn, A. (2018) Origin, dimensions, and distribution of remobilized carbonate deposits in a tectonically active zone, Eocene Thebes Formation, Sinai, Egypt. *Sedimentary Geology*, *372*, 44–63.

Cornacchia, I., Agostini, S. & Brandano, M. (2018) Miocene oceanographic evolution based on the Sr and Nd isotope record of the Central Mediterranean. *Paleoceanography and Paleoclimatology*, *33*(1), 31–47.

Cornacchia, I., Brandano, M. & Agostini, S. (2021) Miocene paleoceanographic evolution of the Mediterranean area and carbonate production changes: a review. *Earth-Science Reviews*, *221*, 103785.

Crabbe, M.J.C. (2008) Climate change, global warming and coral reefs: modelling the effects of temperature. *Computational Biology and Chemistry*, *32*(5), 311–314.

Daraei, M., Amini, A. & Ansari, M. (2015) Facies analysis and depositional environment study of the mixed carbonate–evaporite Asmari Formation (Oligo-Miocene) in the sequence stratigraphic framework, NW Zagros, Iran. *Carbonates and evaporites*, *30*(3), 253–272.

Dercourt, J., Gaetani, M., Vrielynk, B., Barrier, E., Biju-Duval, B., Brunet, M.F., Cadet, J.P, Crasquin, S. & Sandulescu, M. (2000) Atlas peri-Tethys, Palaeogeographical maps.

Dill, M.A., Seyrafian, A. & Vaziri-Moghaddam, H. (2012) Palaeoecology of the Oligocene-Miocene Asmari formation in the Dill anticline (Zagros Basin, Iran). *Neues Jahrbuch für Geologie und Paläontologie-Abhandlungen*, *263*, 167–184.

Dill, M.A., Vaziri-Moghaddam, H., Seyrafian, A. & Behdad, A. (2018) Oligo-Miocene carbonate platform evolution in the northern margin of the Asmari intra-shelf basin, SW Iran. *Marine and Petroleum Geology*, *92*, 437–461.

Dill, M.A., Vaziri-Moghaddam, H., Seyrafian, A., Behdad, A. & Shabafrooz, R. (2020) A review of the oligo–Miocene larger benthic foraminifera in the Zagros basin, Iran: new insights into biozonation and palaeogeographical maps. *Revue de Micropaleontologie*, *66*, 100408.

Dishon, G., Grossowicz, M., Krom, M., Guy, G., Gruber, D.F. & Tchernov, D. (2020) Evolutionary traits that enable scleractinian corals to survive mass extinction events. *Scientific Reports*, *10*(1), 1–10.

Efron, B. (1979) Bootstrap methods: another look at the jackknife. *The Annals of Statistics*, *7*, 1–26.

Esteban, M. (1979) Significance of the upper Miocene coral reefs of the western Mediterranean. *Palaeogeography, Palaeoclimatology, Palaeoecology*, *29*, 169–188.

Esteban, M. (1996) An overview of of Miocene reefs from Mediterranean areas: general trends and facies models. In: Franseen, E.K., Esteban, M., Ward, W.C. & Rouchy, J.M. (Eds.) *Models for carbonate stratigraphy, from Miocene reef complex of the Mediterranean area. Concepts in sedimentology and paleontology 5*. Tulsa, OK: Society for Sedimentary Geology, pp. 3–53.

Fahad, M., Khan, M.A., Hussain, J., Ahmed, A. & Yar, M. (2021) Microfacies analysis, depositional settings and reservoir investigation of Early Eocene Chorgali Formation exposed at Eastern Salt Range, Upper Indus Basin, Pakistan. *Carbonates and Evaporites*, *36*(3), 1–18.

Farouk, S., Ahmad, F. & Smadi, A.A. (2013) Stratigraphy of the Middle Eocene–Lower Oligocene successions in northwestern and eastern Jordan. *Journal of Asian Earth Sciences*, *73*, 396–408.

Fine, M. & Tchernov, D. (2007) Scleractinian coral species survive and recover from decalcification. *Science*, *315*(5820), 1811.

Flügel, E. (2004) *Microfacies of carbonate rocks*. Berlin, Heidelberg: Springer.

Gaetani, M., Nicora, A., Premoli-Silva, I., Fois, E., Garzanti, E. & Tintori, A. (1983) Upper cretaceous and Paleocene in Zanskar range (NW Himalaya). *Rivista Italiana di Paleontologia e Stratigrafia*, *89*, 81–118.

Garzanti, E., Al-Juboury, A.I., Zoleikhaei, Y., Vermeesch, P., Jotheri, J., Akkoca, D.B., Allen, M., Andò, S., Limonta, M., Padoan, M., Resentini, A., Rittner, M. & Vezzoli, G. (2016) The Euphrates-Tigris-Karun river system: provenance, recycling and dispersal of quartz-poor foreland-basin sediments in arid climate. *Earth-Science Reviews*, *162*, 107–128.

Geel, T. (2000) Recognition of stratigraphic sequences in carbonate platform and slope deposits: empirical models based on microfacies analysis of Palaeogene deposits in southeastern Spain. *Palaeogeography, Palaeoclimatology, Palaeoecology*, *155*(3–4), 211–238.

Ghaedi, M., Johnson, K. & Yazdi, M. (2016) Paleoenvironmental conditions of Early Miocene corals, western Makran, Iran. *Arabian Journal of Geosciences*, *9*(17), 1–20.

Ghafur, A.A. (2015) Integrated depositional model of the carbonate Kirkuk group of southern Kurdistan-Iraq. *Journal of Natural Science Research*, *5*, 79–106.

Ghazi, S., Sharif, S., Zafar, T., Riaz, M., Haider, R. & Hanif, T. (2020) Sedimentology and stratigraphic evolution of the Early Eocene Nammal Formation, Salt Range, Pakistan. *Stratigraphy and Geological Correlation*, *28*(7), 745–764.

GholamiZadeh, P., Hu, X., Garzanti, E. & Adabi, M.H. (2021) Constraining the timing of Arabia-Eurasia collision in the Zagros orogen by sandstone provenance (Neyriz, Iran). *GSA Bulletin*, *134*, 1793–1810. https://doi.org/10.1130/B35950

Granier, B. (2012) The contribution of calcareous green algae to the production of limestones: a review. *Geodiversitas*, *34*(1), 35–60.

Hadi, M., Less, G. & Vahidinia, M. (2019) Eocene larger benthic foraminifera (alveolinids, nummulitids, and orthophragmines) from the eastern Alborz region (NE Iran): taxonomy and biostratigraphy implications. *Revue de Micropaleontologie*, *63*, 65–84.

Hadi, M., Mosaddegh, H. & Abbassi, N. (2016) Microfacies and biofabric of nummulite accumulations (Bank) from the Eocene deposits of Western Alborz (NW Iran). *Journal of African Earth Sciences*, *124*, 216–233.

Halfar, J. & Mutti, M. (2005) Global dominance of coralline red-algal facies: a response to Miocene oceanographic events. *Geology*, *33*, 481–484.

Hallock, P. (1997) Reefs and reef limestones in earth history. In: Birkeland, C. (Ed.) *Life and death of coral reefs*. New York: Chapman and Hall, pp. 13–42.

Hallock, P. & Seddighi, M. (2022) Why did some larger benthic foraminifera become so large and flat? *Sedimentology*, *69*(1), 74–87.

Hanif, M., Imraz, M., Ali, F., Haneef, M., Saboor, A., Iqbal, S. & Ahmad, S. (2014) The inner ramp facies of the Thanetian Lockhart formation, western salt range, Indus Basin, Pakistan. *Arabian Journal of Geosciences*, *7*(11), 4911–4926.

Heidari, A., Mahboubi, A., Moussavi-Harami, R., Gonzalez, L. & Moalemi, S.A. (2014) Biostratigraphy, sequence stratigraphy, and paleoecology of the lower–middle Miocene of northern Bandar Abbas, southeast Zagros basin in south of Iran. *Arabian Journal of Geosciences*, *7*(5), 1829–1855.

Herbert, T.D., Lawrence, K.T., Tzanova, A., Peterson, L.C., Caballero-Gill, R. & Kelly, C.S. (2016) Late Miocene global cooling and the rise of modern ecosystems. *Nature Geoscience*, *9*, 843–847.

Höntzsch, S., Scheibner, C., Guasti, E., Kuss, J., Marzouk, A.M. & Rasser, M.W. (2011) Increasing restriction of the Egyptian shelf during the Early Eocene?—new insights from a southern Tethyan carbonate platform. *Palaeogeography, Palaeoclimatology, Palaeoecology*, *302*(3–4), 349–366.

Hottinger, L. (1982) Larger foraminifera, giant cells with a historical background. *Naturwissenschaften*, *69*(8), 361–371.

Hottinger, L.K. (1983) Neritic macroid genesis: an ecological approach. In: Peryt, T.M. (Ed.) *Coated grains*. Berlin: Springer-Verlag, pp. 38–55.

Hu, X., Garzanti, E., Wang, J., Huang, W., An, W. & Webb, A. (2016) The timing of India-Asia collision onset–facts, theories, controversies. *Earth-Science Reviews*, *160*, 264–299.

Hussein, A.W. (2019) Cyclic hierarchy and depositional sequences of the middle-upper Eocene ramp facies: An example from Beni Suef area, East Nile Valley, Egypt. *Journal of African Earth Sciences*, *149*, 307–333.

Hussein, D., Collier, R., Lawrence, J.A., Rashid, F., Glover, P.W.J., Lorinczi, P. & Baban, D.H. (2017) Stratigraphic correlation and paleoenvironmental analysis of the hydrocarbon-bearing Early Miocene Euphrates and Jeribe formations in the Zagros folded-thrust belt. *Arabian Journal of Geosciences*, *10*(24), 1–15.

Ishaq, M., Jan, I.U., Hanif, M. & Awais, M. (2019) Microfacies and diagenetic studies of the early Eocene Sakesar Limestone, Potwar Plateau, Pakistan: approach of reservoir evaluation using outcrop analogue. *Carbonates and Evaporites*, *34*(3), 623–656.

James, N.P. (1997) The cool-water carbonate depositional realm. In: James, N.P. & Clarke, J.A.D. (Eds.), *Cool-water carbonates*, vol. 56. SEPM Special Publication, Tulsa, OK: SEPM Society for Sedimentary Geology, pp. 1–22.

Jauhri, A.K., Misra, P.K., Kishore, S. & Singh, S.K. (2006) Larger foraminiferal and calcareous algal facies in the Lakadong Formation of the South Shillong Plateau, NE India. *Journal of the Palaeontological Society of India*, *51*(2), 51–61.

Jiang, J., Hu, X., Li, J., BouDagher-Fadel, M. & Garzanti, E. (2021) Discovery of the Paleocene-Eocene thermal maximum in shallow-marine sediments of the Xigaze forearc basin, Tibet: a record of enhanced extreme precipitation and siliciclastic sediment flux. *Palaeogeography, Palaeoclimatology, Palaeoecology*, *562*, 110095.

Johnson, K.G., Jackson, J.B. & Budd, A.F. (2008) Caribbean reef development was independent of coral diversity over 28 million years. *Science*, *319*(5869), 1521–1523.

Joudaki, M., Asnavandi, H., Panah, F.M. & Baghbani, D. (2020) The regional facies analysis and depositional environments of the Oligocene and lower Miocene deposits; Zagros Basin, SW of Iran. *Carbonates and Evaporites*, *35*(2), 1–18.

Kahsnitz, M. (2017) Paleocene to lower Eocene sediments of the eastern Neo-Tethyan Ocean: sedimentary and geodynamic evolution as well as biostratigraphy of the larger benthic foraminifera Lockhartia and the genesis of nodular limestones. Doctoral dissertation, Universität Bremen.

Kamran, M., Frontalini, F., Xi, D., Papazzoni, C.A., Jafarian, A., Latif, K., Jiang, T., Mirza, K., Song, H. & Wan, X. (2021) Larger benthic foraminiferal response to the PETM in the Potwar Basin (eastern Neotethys, Pakistan). *Palaeogeography, Palaeoclimatology, Palaeoecology*, *575*, 110450.

Khan, M., Khan, M.A., Shami, B.A. & Awais, M. (2018) Microfacies analysis and diagenetic fabric of the Lockhart Limestone exposed near Taxila, Margalla Hill range, Punjab, Pakistan. *Arabian Journal of Geosciences*, *11*(2), 1–15.

Khitab, U., Umar, M. & Jamil, M. (2020) Microfacies, diagenesis and hydrocarbon potential of Eocene carbonate strata in Pakistan. *Carbonates and Evaporites*, *35*(3), 1–15.

Kiessling, W., Flügel, E. & Golonka, J. (1999) Paleo reef maps: evaluation of a comprehensive database on phanerozoic reefs. *American Association of Petroleum Geologists Bullettin*, *83*, 1552–1587.

Kiessling, W., Flügel, E., Golonka, J. 2002. *Phanerozoic reef patterns*. SEPM Special Publication, Tulsa, OK: Society for Sedimentary Geology (SEPM), 775 pp.

Kuss, J. & Boukhary, M.A. (2008) A new upper Oligocene marine record from northern Sinai (Egypt) and its paleogeographic context. *GeoArabia*, *13*(1), 59–84.

Langer, M.R. & Hottinger, L. (2000) Biogeography of selected" larger" foraminifera. *Micropaleontology*, *46*, 105–126.

Less, G., Frijia, G., Özcan, E., Saraswati, P.K., Parente, M. & Kumar, P. (2018) Nummulitids, lepidocyclinids and Sr-isotope data from the Oligocene of Kutch (western India) with chronostratigraphic and paleobiogeographic evaluations. *Geodinamica Acta*, *30*(1), 183–211.

Leutenegger, S. (1984) Symbiosis in benthic foraminifera; specificity and host adaptations. *The Journal of Foraminiferal Research*, *14*, 16–35.

Li, J., Hu, X., Garzanti, E., An, W. & Wang, J. (2015) Paleogene carbonate microfacies and sandstone provenance (Gamba area, South Tibet): stratigraphic response to initial India–Asia continental collision. *Journal of Asian Earth Sciences*, *104*, 39–54.

Li, J., Hu, X., Zachos, J.C., Garzanti, E. & BouDagher-Fadel, M. (2020) Sea level, biotic and carbon-isotope response to the Paleocene–Eocene thermal maximum in Tibetan Himalayan platform carbonates. *Global and Planetary Change*, *194*, 103316.

Lokier, S.W., Wilson, M.E. & Burton, L.M. (2009) Marine biota response to clastic sediment influx: a quantitative approach. *Palaeogeography, Palaeoclimatology, Palaeoecology*, *281*(1–2), 25–42.

López-Pérez, A. (2017) Revisiting the Cenozoic history and the origin of the eastern Pacific coral fauna. In: Glynn, P., Manzello, D. & Enochs, I. (Eds.) *Coral reefs of the eastern tropical Pacific*. Dordrecht: Springer, pp. 39–57.

López-Pérez, R.A. (2005) The Cenozoic hermatypic corals in the eastern Pacific: history of research. *Earth-Science Reviews*, *72*(1–2), 67–87.

Mahboubi, A., Moussavi-Harami, R., Lasemi, Y. & Brenner, R.L. (2001) Sequence stratigraphy and sea level history of the upper Paleocene strata in the Kopet-Dagh basin, northeastern Iran. *AAPG Bulletin*, *85*(5), 839–859.

Mahyad, M., Safari, A., Vaziri-Moghaddam, H. & Seyrafian, A. (2019) Biofacies, taphofacies, and depositional environments in the north of Neotethys seaway (Qom Formation, Miocene, Central Iran). *Russian Geology and Geophysics*, *60*(12), 1368–1384.

Marshall, A.T. & Clode, P. (2004) Calcification rate and the effect of temperature in a zooxanthellate and an azooxanthellate scleractinian reef coral. *Coral Reefs*, *23*(2), 218–224.

Martín-Martín, M., Guerrera, F., Tosquella, J. & Tramontana, M. (2020) Paleocene-lower Eocene carbonate platforms of westernmost Tethys. *Sedimentary Geology*, *404*, 105674.

Mattern, F. & Bernecker, M. (2019) A shallow marine clinoform system in limestones (Paleocene/Eocene Jafnayn Formation, Oman): geometry, microfacies, environment and processes. *Carbonates and Evaporites*, *34*(1), 101–113.

Miller, K.G., Browning, J.V., Schmelz, W.J., Kopp, R.E., Mountain, G.S. & Wright, J.D. (2020) Cenozoic sea-level and cryospheric evolution from deep-sea geochemical and continental margin records. *Science Advances*, *6*(20), eaaz1346.

Moghaddam, H.V., Seyrafian, A. & Taraneh, P. (2002) Biofacies and sequence stratigraphy of the Eocene succession, at Hamzeh-Ali area, north-central Zagros, Iran. *Carbonates and Evaporites*, *17*(1), 60–67.

Mohammadi, E. (2020) Sedimentary facies and depositional environments of the Oligocene–early Miocene marine Qom formation, Central Iran Back-Arc Basin, Iran (northeastern margin of the Tethyan seaway). *Carbonates and Evaporites*, *35*(1), 1–29.

Mohammadi, E., Hasanzadeh-Dastgerdi, M., Ghaedi, M., Dehghan, R., Safari, A., Vaziri-Moghaddam, H., Baizidi, C., Vaziri, M. & Sfidari, E. (2013) The Tethyan Seaway Iranian Plate Oligo-Miocene deposits (the Qom Formation): distribution of Rupelian (Early Oligocene) and evaporate deposits as evidences for timing and trending of opening and closure of the Tethyan Seaway. *Carbonate Evaporite*, *28*, 321–345.

Mohammadi, E., Safari, A., Vaziri-Moghaddam, H., Vaziri, M.R. & Ghaedi, M. (2011) Microfacies analysis and paleoenviornmental interpretation of the Qom formation, south of the Kashan, Central Iran. *Carbonates and Evaporites*, *26*(3), 255–271.

Mossadegh, Z.K., Haig, D.W., Allan, T., Adabi, M.H. & Sadeghi, A. (2009) Salinity changes during late Oligocene to early Miocene Asmari formation deposition, Zagros mountains, Iran. *Palaeogeography, Palaeoclimatology, Palaeoecology*, *272*(1–2), 17–36.

Nafarieh, E., Boix, C., Cruz-Abad, E., Ghasemi-Nejad, E., Tahmasbi, A. & Caus, E. (2019) Imperforate larger benthic foraminifera from shallow-water carbonate facies (middle and late Eocene), Zagros Mountains, Iran. *Journal of Foraminiferal Research*, *49*(3), 275–302.

Nafarieh, E., Vaziri-Moghaddam, H., Taheri, A. & Ghabeishavi, A. (2012) Biofacies and palaeoecology of the Jahrum Formation in Lar area, Zagros Basin, (SW Iran). *Iranian Journal of Science and Technology*, *36*(A1), 51.

Naveed, A. & Chaudhry, M.N. (2008) Geology of Hettangian to middle Eocene rocks of Hazara and Kashmir basins, northwest lesser Himalayas, Pakistan. *Geological Bulletin of Panjab University*, *43*, 131–152.

Nebelsick, J.H., Rasser, M.W. & Bassi, D. (2005) Facies dynamics in Eocene to Oligocene circumalpine carbonates. *Facies*, *51*(1), 197–217.

Noorian, Y., Moussavi-Harami, R., Reijmer, J.J., Mahboubi, A., Kadkhodaie, A. & Omidpour, A. (2021) Paleo-facies distribution and sequence stratigraphic architecture of the Oligo-Miocene Asmari carbonate platform (Southeast Dezful Embayment, Zagros Basin, SW Iran). *Marine and Petroleum Geology*, *128*, 105016.

Özcan, E., Hanif, M., Ali, N. & Yücel, A.O. (2015) Early Eocene orthophragminids (foraminifera) from the type-locality of Discocyclina ranikotensis Davies, 1927, Thal, NW Himalayas, Pakistan: insights into the orthophragminid palaeobiogeography. *Geodinamica Acta*, *27*(4), 267–299.

Özcan, E., Saraswati, P.K., Yücel, A.O., Ali, N. & Hanif, M. (2018) Bartonian orthophragminids from the Fulra limestone (Kutch, W India) and coeval units in Sulaiman range, Pakistan: a synthesis of shallow benthic zone (SBZ) 17 for the Indian subcontinent. *Geodinamica Acta*, *30*(1), 137–162.

Perrin, C. (1992) Signification écologique des foraminifères acervulinidés et leur rôle dans la formation de faciès récifaux et organogènes depuis le Paléocène. *Geobios*, *25*(6), 725–751.

Perrin, C. (2009) Solenomeris: from biomineralization patterns to diagenesis. *Facies*, *55*(4), 501–522.

Perrin, C. & Bosellini, F.R. (2012) Paleobiogeography of scleractinian reef corals: changing patterns during the Oligocene–Miocene climatic transition in the Mediterranean. *Earth-Science Reviews*, *111*(1–2), 1–24.

Perrin, C. and Kiessling, W. (2012) Latitudinal trends in Cenozoic reef patterns and their relationship to climate. In: Mutti, M., Piller, W., Betzler, C. (Eds.), *Carbonate systems during the Oligocene-Miocene climatic transition*, vol. *42*. Oxford, UK: Wiley-Blackwell. International Association of Sedimentologists Special Publications, pp. 17–34.

Perry, O.R. & Choquette, P.W. (1985) *Carbonate petroleum reservoirs*. New York: Springer.

Pomar, L., Baceta, J.I., Hallock, P., Mateu-Vicens, G. & Basso, D. (2017) Reef building and carbonate production modes in the west-central Tethys during the Cenozoic. *Marine and Petroleum Geology*, *83*, 261–304.

Pomar, L., Bassant, P., Brandano, M., Ruchonnet, C. & Janson, X. (2012) Impact of carbonate producing biota on platform architecture:

insights from Miocene examples of the Mediterranean region. *Earth-Science Reviews*, *113*(3–4), 186–211.

Pomar, L., Brandano, M. & Westphal, H. (2004) Environmental factors influencing skeletal grain sediment associations: a critical review of Miocene examples from the western Mediterranean. *Sedimentology*, *51*(3), 627–651.

Pomar, L. & Hallock, P. (2007) Changes in coral-reef structure through the Miocene in the Mediterranean province: adaptive versus environmental influence. *Geology*, *35*(10), 899–902.

Rahmani, A., Vaziri-Moghaddam, H., Taheri, A. & Ghabeishavi, A. (2009) A model for the paleoenvironmental distribution of larger foraminifera of Oligocene–Miocene carbonate rocks at Khaviz Anticline, Zagros Basin, SW Iran. *Historical Biology*, *21*(3–4), 215–227.

Rasser, M.W. and Piller, W.E. (1997) Depth distribution of calcareous encrusting associations in the northern Red Sea (Safaga, Egypt) and their geological implications. Proceedings of the 8th international Coral Reef Symposium, 743–748.

Rasser, W.M. (1994) Facies and palaeoecology of rhodoliths and acervulinid macroids in the Eocene of the Krappfeld (Austria). *Beiträge zur Paläontologie*, *19*, 191–217.

Renema, W. (2018) Terrestrial influence as a key driver of spatial variability in large benthic foraminiferal assemblage composition in the central Indo-Pacific. *Earth-Science Reviews*, *177*, 514–544.

Reuter, M., Piller, W.E., Harzhauser, M., Kroh, A. & Bassi, D. (2008) Termination of the Arabian shelf sea: stacked cyclic sedimentary patterns and timing (Oligocene/Miocene, Oman). *Sedimentary Geology*, *212*(1–4), 12–24.

Reuter, M., Piller, W.E., Harzhauser, M., Mandic, O., Berning, B., Rogl, F., Kroh, A., Aubry, M.P., Wielandt-Schuster, U. & Hamedani, A. (2009) The oligo−/Miocene Qom Formation (Iran): evidence for an early Burdigalian restriction of the Tethyan Seaway and closure of its Iranian gateways. *International Journal of Earth Sciences*, *98*(3), 627–650. https://doi.org/10.1007/s00531-007-0269-9

Riosmena-Rodríguez, R. (2017) Natural history of Rhodolith/Maërl beds: their role in near-shore biodiversity and management. In: Riosmena-Rodríguez R., Nelson W. & Aguirre J. (Eds), *Rhodolith/Maërl beds: a global perspective. Coastal research library*, vol. 15, 3–27. Cham, Switzerland: Springer.

Robertson, A.H.F., Parlak, O. & Ustaömer, T. (2012) Overview of the Palaeozoic–Neogene evolution of Neotethys in the Eastern Mediterranean region (Southern Turkey, Cyprus, Syria). *Petroleum Geoscience*, *18*, 381–404.

Rögl, F. (1999) Mediterranean and Paratethys facts and hypotheses of an Oligocene to Miocene paleogeography (short overview). *Geologica Carpathica*, *50*, 339–349.

Roozpeykar, A., Maghfouri-Moghaddam, I., Yazdi, M. & Yousefi-Yegane, B. (2019) Facies and paleoenvironmental reconstruction of Early-Middle Miocene deposits in the north-west of the Zagros Basin. *Iran Geologica Carpathica*, *70*(1), 75–87.

Roozpeykar, A. & Moghaddam, I.M. (2016) Benthic foraminifera as biostratigraphical and paleoecological indicators: an example from oligo-Miocene deposits in the SW of Zagros basin, Iran. *Geoscience Frontiers*, *7*(1), 125–140.

Rosenfeld, A. & Hirsch, F. (2005) The Paleocene – Eocene of Israel. In: Hall, J.K., Krasheninnikov, V.A., Hirsch, F., Benjamini, C. & Flexer, A. (Eds.) *Geological framework of the levant – Volume II: The Levantine Basin and Israel*. Jerusalem: Historical Productions-Hall, pp. 437–458.

Sadeghi, R., Vaziri-Moghaddam, H. & Taheri, A. (2011) Microfacies and sedimentary environment of the Oligocene sequence (Asmari Formation) in Fars sub-basin, Zagros Mountains, Southwest Iran. *Facies*, *57*(3), 431–446.

Sadooni, F.N. & Alsharhan, A.S. (2019) Regional stratigraphy, facies distribution, and hydrocarbons potential of the Oligocene strata across the Arabian plate and Western Iran. *Carbonates and Evaporites*, *34*(4), 1757–1770.

Safari, A., Ghanbarloo, H., Mansoury, P. & Esfahani, M.M. (2020) Reconstruction of the depositional sedimentary environment of Oligocene deposits (Qom formation) in the Qom Basin (northern Tethyan Seaway), Iran. *Geologos*, *26*(2), 93–111.

Sallam, E., Wanas, H.A. & Osman, R. (2015) Stratigraphy, facies analysis and sequence stratigraphy of the Eocene succession in the Shabrawet area (north Eastern Desert, Egypt): an example for a tectonically influenced inner ramp carbonate platform. *Arabian Journal of Geosciences*, *8*(12), 10433–10458.

Sarkar, S. (2016) Early Eocene calcareous algae and benthic foraminifera from Meghalaya, NE India: a new record of microfacies and palaeoenvironment. *Journal of the Geological Society of India*, *88*(3), 281–294.

Sarkar, S. (2017) Microfacies analysis of larger benthic foraminifera-dominated middle Eocene carbonates: a palaeoenvironmental case study from Meghalaya, NE India (eastern Tethys). *Arabian Journal of Geosciences*, *10*(5), 1–13.

Sarkar, S. (2018) The enigmatic Palaeocene-Eocene coralline *Distichoplax*: approaching the structural complexities, ecological affinities and extinction hypotheses. *Marine Micropaleontology*, *139*, 72–83.

Schaub, H., Benjamini, C. and Moshkovitz, S. (1995) The biostratigraphy of the Eocene of Israel: nummulites Planktic Foraminifera and Calcareous Nannofossils. Kommission der Schweizerischen Paläontologischen Abhandlungen, 58 p.

Scheibner, C., Kuss, J. & Marzouk, A.M. (2000) Slope sediments of a Paleocene ramp-to-basin transition in NE Egypt. *International Journal of Earth Sciences: Geologische Rundschau*, *88*(4), 708–724.

Scheibner, C., Reijmer, J.J.G., Marzouk, A.M., Speijer, R.P. & Kuss, J. (2003) From platform to basin: the evolution of a Paleocene carbonate margin (Eastern Desert, Egypt). *International Journal of Earth Sciences*, *92*(4), 624–640.

Scheibner, C. & Speijer, R.P. (2008) Late Paleocene–early Eocene Tethyan carbonate platform evolution – a response to long-and short-term paleoclimatic change. *Earth-Science Reviews*, *90*(3–4), 71–102.

Schlager, W. (2003) Benthic carbonate factories of the Phanerozoic. *International Journal of Earth Sciences*, *92*, 445–464.

Scotese, C.R. (2014a) Atlas of Paleogene paleogeographic maps (Mollweide projection), maps 8–15, Volume 1. The Cenozoic, PALEOMAP Atlas for ArcGIS, PALEOMAP Project, Evanston, IL.

Scotese, C.R. (2014b) Atlas of Neogene paleogeographic maps (Mollweide projection), maps 1–7, volumes 1. The Cenoaoic, PALEOMAP Atlas for ArcGIS, PALEOMAP Project, Evanston, IL.

Sengupta, S., Volgushev, S. & Shao, X. (2016) A subsampled double bootstrap for massive data. *Journal of the American Statistical Association*, *111*(515), 1222–1232.

Serra-Kiel, J., Hottinger, L., Caus, E., Drobne, K., Ferrandez, C., Jauhri, A.K., Less, G., Pavlovec, R., Pignatti, J., Samso, J.M., Schaub, H., Sirel, E., Strougo, A., Tambareau, Y., Tosquella, J. & Zakrevskaya,

E. (1998) Larger foraminiferal biostratigraphy of the Tethyan. *Bulletin de la Société géologique de France*, *169*, 281–299.

Seyrafian, A. & Toraby, H. (2005) Petrofacies and sequence stratigraphy of the Qom Formation (Late Oligocene-Early Miocene?), north of Nain, southern trend of central Iranian Basin. *Carbonates and Evaporites*, *20*(1), 82–90.

Shabafrooz, R., Mahboubi, A., Vaziri-Moghaddam, H., Ghabeishavi, A. & Moussavi-Harami, R. (2015) Depositional architecture and sequence stratigraphy of the oligo–miocene Asmari platform; southeastern Izeh zone, Zagros Basin, Iran. *Facies*, *61*(1), 1–32.

Sissakian, V.K. (2013) Geological evolution of the Iraqi Mesopotamia foredeep, inner platform and near surroundings of the Arabian plate. *Journal of Asian Earth Sciences*, *72*, 152–163.

Stanley, S.M. (2006) Influence of seawater chemistry on biomineralization throughout phanerozoic time: paleontological and experimental evidence. *Palaeogeography, Palaeoclimatology, Palaeoecology*, *232*(2–4), 214–236.

Steinthorsdottir, M., Coxall, H.K., de Boer, A.M., Huber, M., Barbolini, N., Bradshaw, C.D., Burls, N.J., Feakins, S.J., Gasson, E., Henderiks, J., Holbourn, A., Kiel, S., Kohn, M.J., Knorr, G., Kürschner, W.M., Lear, C., Liebrand, D., Lunt, D.J., Mörs, T., Pearson, P.N., Pound, M.J., Stoll, H. and Strömberg, C.A.E. (2020) The Miocene: the future of the past. *Paleoceanography and Paleoclimatology*, *36*, 1–71.

Swati, M.A.F., Haneef, M., Ahmad, S., Naveed, Y., Zeb, W., Akhtar, N. & Owais, M. (2013) Biostratigraphy and depositional environments of the early Eocene Margalla Hill limestone, Kohala-Bala area, Haripur, Hazara fold-Thrust Belt, Pakistan. *Journal of Himalayan Earth Sciences*, *46*(2), 65.

Taheri, A., Vaziri-Moghaddam, H. & Seyrafian, A. (2008) Relationships between foraminiferal assemblages and depositional sequences in Jahrum formation, Ardal area (Zagros Basin, SW Iran). *Historical Biology*, *20*(3), 191–201.

Titelboim, D., Almogi-Labin, A., Herut, B., Kucera, M., Asckenazi-Polivoda, S. & Abramovich, S. (2019) Thermal tolerance and range expansion of invasive foraminifera under climate changes. *Scientific Reports*, *9*(1), 1–5.

Tomás, S., Frijia, G., Bömelburg, E., Zamagni, J., Perrin, C. & Mutti, M. (2016) Evidence for seagrass meadows and their response to paleoenvironmental changes in the early Eocene (Jafnayn formation, Wadi Bani Khalid, N Oman). *Sedimentary Geology*, *341*, 189–202.

Torfstein, A. & Steinberg, J. (2020) The oligo–Miocene closure of the Tethys Ocean and evolution of the proto-Mediterranean Sea. *Scientific Reports*, *10*(1), 1–10.

Tucker, M.E. & Wright, V.P. (1990) *Carbonate sedimentology*. Oxford: Blackwell, pp. 1–496.

Van Buchem, F.S.P., Allan, T.L., Laursen, G.V., Lotfpour, M., Moallemi, A., Monibi, S., Motiei, H., Pickard, N.A.H., Tahmasbi, A.R., Vedrenne, V. and Vincent, B. (2010) Regional stratigraphic architecture and reservoir types of the oligo-Miocene deposits in the Dezful embayment (Asmari and Pabdeh Formations) SW Iran. In: Van Buchem, F.S.P., Gerdes, K.D., & Esteban, M. (Eds.), *Mesozoic and Cenozoic carbonate systems of the Mediterranean and the Middle East: stratigraphic and diagenetic reference models*. Geological Society of London, Special Publications, London: Geological Society, *329*, 219–263.

Vaziri-Moghaddam, H., Kalanat, B. & Taheri, A. (2011) Sequence stratigraphy and depositional environment of the Oligocene deposits at Firozabad section, southwest of Iran based on microfacies analysis. *Geopersia*, *1*(1), 71–152.

Vaziri-Moghaddam, H., Kimiagari, M. & Taheri, A. (2006) Depositional environment and sequence stratigraphy of the Oligo-Miocene Asmari Formation in SW Iran. *Facies*, *52*(1), 41–51.

Vaziri-Moghaddam, H., Seyrafian, A., Taheri, A. & Motiei, H. (2010) Oligocene-Miocene ramp system (Asmari Formation) in the NW of the Zagros basin, Iran: microfacies, paleoenvironment and depositional sequence. *Revista mexicana de ciencias geológicas*, *27*(1), 56–71.

Whittle, G.L., Alsharhan, A.S. & El Deeb, W.M.Z. (1995) Biolithofacies and diagenesis in the early-middle oligocene of Abu Dhabi, United Arab Emirates. *Carbonates and Evaporites*, *10*(1), 54–64.

Willems, H., Zhou, Z., Zhang, B.G. & Gräfe, K.U. (1996) Stratigraphy of the upper cretaceous and lower tertiary strata in the Tethyan Himalayas of Tibet (Tingri area, China). *Geologische Rundschau*, *85*(4), 723–754.

Wilson, M.E.J. (2008) Global and regional influences on equatorial shallow-marine carbonates during the Cenozoic. *Palaeogeography Palaeoclimatology Palaeoecology*, *265*, 262–274.

Wilson, M.E.J. & Vecsei, A. (2005) The apparent paradox of abundant foramol facies in low latitudes: their environmental significance and effect on platform development. *Earth-Science Reviews*, *69*(1–2), 133–168.

Wright, V.P. & Burchette, T.P. (1996) Shallow-water carbonate environments. In: Reading, H.G. (Ed.) *Sedimentary environments*. Oxford: Blackwell, pp. 325–394.

Yazdi-Moghadam, M., Sadeghi, A., Adabi, M.H. & Tahmasbi, A. (2018a) Foraminiferal biostratigraphy of the lower Miocene Hamzian and Arashtanab sections (NW Iran), northern margin of the Tethyan Seaway. *Geobios*, *51*(3), 231–246.

Yazdi-Moghadam, M., Sadeghi, A., Adabi, M.H. & Tahmasbi, A. (2018b) Stratigraphy of the lower Oligocene nummulitic limestones, north of Sonqor (Nw Iran). *Rivista Italiana di Paleontologia e Stratigrafia*, *124*(2), 407–416.

Yazdi-Moghadam, M., Sarfi, M., Ghasemi-Nejad, E., Sadeghi, A. & Sharifi, M. (2021) Early Miocene larger benthic foraminifera from the northwestern Tethyan seaway (NW Iran): new findings on shallow benthic zone 25. *International Journal of Earth Sciences*, *110*(2), 719–740.

Zachos, J., Pagani, M., Sloan, L., Thomas, E. & Billups, K. (2001) Trends, rhythms, and aberrations in global climate 65 ma to present. *Science*, *292*(5517), 686–693.

Zhang, Q., Willems, H. & Ding, L. (2013) Evolution of the Paleocene-early Eocene larger benthic foraminifera in the Tethyan Himalaya of Tibet, China. *International Journal of Earth Sciences*, *102*(5), 1427–1445.

Ziegler, A.M. (2001) Late Permian to Holocene paleofacies evolution of the Arabian plate and its hydrocarbon occurrences. *GeoArabia*, *6*(3), 445–504.

Zoeram, F.Z., Vahidinia, M., Sadeghi, A., Mahboubi, A. & Bakhtiar, H.A. (2015) Larger benthic foraminifera: a tool for biostratigraphy, facies analysis and paleoenvironmental interpretations of the oligo-Miocene carbonates, NW central Zagros Basin, Iran. *Arabian Journal of Geosciences*, *2*(8), 931–949.

Zohdi, A., Mousavi-Harami, R., Ali Moallemi, S., Mahboubi, A. & Immenhauser, A. (2013) Evolution, paleoecology and sequence

architecture of an Eocene carbonate ramp, southeast Zagros Basin, Iran. *GeoArabia*, *18*(4), 49–80.

SUPPORTING INFORMATION

Additional supporting information can be found online in the Supporting Information section at the end of this article.

How to cite this article: Coletti, G., Commissario, L., Mariani, L., Bosio, G., Desbiolles, F., Soldi, M. & Bialik, O. M. (2022). Palaeocene to Miocene southern Tethyan carbonate factories: A meta-analysis of the successions of South-western and Western Central Asia. *The Depositional Record*, *8*, 1031–1054. https://doi.org/10.1002/dep2.204